



The long-term impacts of climate and fire on catchment processes and aquatic ecosystem response in Tasmania, Australia

Kristen K. Beck ^{a,b,*}, Michael-Shawn Fletcher ^b, Patricia S. Gadd ^c, Henk Heijnis ^c, Krystyna M. Saunders ^c, Atun Zawadzki ^c

^a Lincoln Centre for Water and Planetary Health, School of Geography, University of Lincoln, Brayford Pool, Lincoln, United Kingdom

^b School of Geography, University of Melbourne, Parkville, Victoria, Australia

^c Australian Nuclear Science and Technology Organisation, Lucas Heights, New South Wales, Australia



ARTICLE INFO

Article history:

Received 11 March 2019

Received in revised form

12 August 2019

Accepted 19 August 2019

Available online 30 August 2019

Keywords:

Holocene

Climate

Fire

Diatoms

Tasmania

Charcoal

XRF geochemistry

Pollen

Carbon/Nitrogen

Palaeoecology

ABSTRACT

The impacts of fire and climate on freshwater ecosystems are not well understood, masking the potential impacts of anthropogenic climate change on these systems. A 9200 year Holocene record of sedimentary Carbon/Nitrogen, x-ray fluorescence, charcoal, pollen, and diatoms preserved within a freshwater lake in Tasmania was used to understand the influences of climate variability and fire on aquatic ecosystem response. Western Tasmania is a cool temperate environment where fire occurrence is driven by hydroclimate. High rainfall during the early to mid-Holocene drove an increase in rainforest and peat in the absence of fire, resulting in an oligotrophic and turbid aquatic environment. This also resulted in leaching of humic acid from the catchment, increasing acidity and dystrophy. The onset of a drier, more variable hydroclimate from the mid-to-late Holocene drove lower lake levels and a shift to the dominant planktonic diatom species, *Discostella stelligera*, the result of the unusual bathymetry of Lake Vera where planktonic diatoms increase with lower lake levels. Further drying caused burning of the rainforest (at ca. 2.3 ka) and increased terrigenous deposition into the lake, leading to a productive, alkaline and disturbed diatom community. Repeated fire disturbance resulted in increased inorganic material deposition, the removal of nutrient rich peat, and an invasion of ferns and sclerophyll vegetation. These fire-driven catchment changes caused a shift in the diatom community to low productivity, oligotrophic and acidic assemblages, likely due to restricted light availability and nutrient uptake by increased deposition of terrigenous material. Therefore, the aquatic ecosystem is responding to climate-mediated changes in the terrestrial environment consistent with regional trends in nearby terrestrial-aquatic Holocene records.

© 2019 Elsevier Ltd. All rights reserved.

1. Introduction

Climate is often the overarching control of aquatic ecosystem change, both via direct effects of climate on the aquatic environment and indirect effects through the surrounding terrestrial environment (Beck et al., 2018b; Fritz and Anderson, 2013; Law et al., 2015). A raft of literature details the direct impacts of climatic change on aquatic ecosystem response; however, the role of terrestrial ecosystem dynamics in driving aquatic ecosystem change is less well known (Ball et al., 2010). A case-in-point is the

poorly understood role of fire-driven terrestrial ecosystem processes in governing aquatic ecosystem dynamics. This gap in knowledge exposes a limitation in our capacity to respond, adapt and mitigate the effects of climatic change on aquatic systems in the future, particularly in the context of a predicted (and realised) increase in wildfire in many regions of the world (Harris et al., 2018; Krawchuk et al., 2009; Moritz et al., 2012). To address this knowledge gap, we use a sediment archive record to test the response of the aquatic environment to climate, catchment and fire driven processes in southwest Tasmania, Australia; a region with little knowledge of aquatic ecosystem response to long-term climate variability and where increasing wildfires are a significant threat (Mariani and Fletcher, 2016).

Climate exerts control over vegetation change, nutrient cycling, and soil development at multiple spatial and temporal scales.

* Corresponding author. Lincoln Centre for Water and Planetary Health, School of Geography, University of Lincoln, Brayford Pool, Lincoln, United Kingdom.

E-mail address: kbeck@lincoln.ac.uk (K.K. Beck).

Changes in the terrestrial environment can be propagated into aquatic systems, resulting in a diverse array of effects that include changes in nutrient status, pH, water chemistry, and biotic species composition (Huvane and Whitehead, 1996; Mariani et al., 2018; Neil and Gajewski, 2018; Perren et al., 2017). For example, high rainfall increases rainforest coverage, enhancing nutrient delivery into waterbodies altering lake trophic status (Beck et al., 2018b). Indeed, studies that investigate the response of both terrestrial and aquatic ecosystems to environmental change reveal a remarkably tight coupling in response of these systems to a range of environmental drivers including climate, non-climate-related nutrient dynamics, lake ontogeny, bedrock weathering, erosion, and human impacts (Augustinus et al., 2012; Ball et al., 2010; Beck et al., 2018b; Mills et al., 2017; Neil and Gajewski, 2018; Perren et al., 2017). Despite this growing recognition, there is little understanding of long-term (Holocene) aquatic ecosystem response to climatic change, particularly in the Southern Hemisphere. This knowledge gap is important, given that the ecological recovery time and rate of change of many terrestrial and aquatic systems exceed the observational window of monitoring (neo-) ecological data. Thus, developing a meaningful understanding of how such systems behave requires the collection of long-term (palaeo-) ecological data and hypothesis testing of external and internal drivers of terrestrial-aquatic system trajectories (Battarbee, 2000; Birks and Birks, 2006; Smol, 2010).

Australia is host to one of, if not the, most flammable flora on Earth. Paradoxically, this continent also hosts some of the most fire sensitive and long-lived species living today (Holz et al., 2015). Many of these fire-sensitive ecosystems have been severely impacted by burning over recent centuries, with recent climate change driving an increase in the occurrence and severity of climate-driven wildfires (Mariani and Fletcher, 2016). While the impact of climate change and fire on fire-sensitive vegetation in Australia is relatively well understood from both neo- and palaeoecological studies, very little is known about how fire-driven vegetation change influences aquatic ecosystems on this continent. This lack of knowledge has real implications for the management of aquatic ecosystems in areas vulnerable to the effects of both climate change and changing fire regimes, such as the unique and endangered systems found in the Tasmanian World Heritage Area (DPIPWE, 2016). This area hosts the highest density of freshwater ecosystems in Australia and, while most recent management plans for this region present detailed synopses of the potential impacts of climate change on the terrestrial environment (e.g. increased wildfires and the loss of endemic plant systems), the potential impacts of climate change or fire on aquatic environments, or their mitigation and management strategies, is absent (DPIPWE, 2016).

Fire is a key ecological process in the Australian landscape and has been used as a landscape management tool since the arrival of humans more than 60,000 years ago, radically altering the 'biological furniture' (Bowman, 1998). In the high rainfall west of Tasmania, the timing and location of fires ignited by people resulted in the failure of fire-sensitive rainforest, which have dominated all pre-human interglacial palynofloras, to re-establish across the landscape following the Last Glacial Maximum (Fletcher and Thomas, 2010). Instead, the landscape is dominated by fire-promoted treeless vegetation and eucalypt forest. While humans are the main ignition source in Tasmania (Bowman and Brown, 1986), trends in fire activity inferred from lake sediment archives reveal a strong relationship between centennial to multi-millennial scale fire activity and climate through the Holocene, reflecting the modulation of human burning and climate over long temporal and large spatial scales (Mariani and Fletcher, 2016, 2017; Mariani et al., 2016).

The magnitude and intensity of wildfires are predicted to increase with future rises in temperature, increasing drought stress brought on by climate change (Flannigan et al., 2009; Fox-Hughes et al., 2014). Yet the impacts of fire on terrestrial and aquatic environments are numerous, complex and not well known. The impact of fire on aquatic chemistry is dependent on the vegetation type on the landscape, soil and geology, and the frequency of fire (Birks, 1997; Dunnette et al., 2014; Renberg et al., 1993a). Fire can cause increased erosion of terrestrial material, heavy metals and mobilise nutrients (Korhola et al., 1996; Leys et al., 2016; Smith et al., 2011; White et al., 2006). These terrigenous deposits result in increased allochthonous inputs causing turbid waters, change in light penetration and altered lake chemistry trophic status (Bixby et al., 2015; Klose et al., 2015; Leys et al., 2016; Morris et al., 2015). Alkalisation is a common outcome of frequent burning due to the destruction of the acid humus soil layer and release base cations from ash deposition (Beck et al., 2018a; Birks, 1997; Huvane and Whitehead, 1996; Korhola et al., 1996; Korsman and Segerstrom, 1998). In contrast, little is known regarding the effects of fire on aquatic ecosystems in the Tasmanian landscape, a region shaped by fire. In Tasmania, a long history of research in fire-ecology reveals a pivotal role of fire in shaping the terrestrial environment via the effects of fire on species composition, soil structure and vegetation-soil feedbacks (Bowman and Wood, 2009; Bowman et al., 2011; Fletcher et al., 2015; Jackson, 1968; Murphy et al., 2013; Wood and Bowman, 2012). The limited work on aquatic ecosystem response to fire indicates that aquatic environments are highly sensitive to climate and fire-driven changes in vegetation, principally via changes in the delivery of terrestrial material into aquatic systems that alter within-lake processes, such as nutrient availability, levels of dystrophy, and pH (Beck et al., 2018a, 2018b).

Here, we present a multi-proxy palaeoecological dataset of coupled terrestrial and aquatic ecosystem change from Lake Vera in southwest Tasmania, Australia, spanning the last 9200 years (9.2 kyr). We seek to understand the impacts of climate and fire on aquatic ecosystem change, including important landscape processes that may drive these changes (i.e. vegetation and soil dynamics). We employ diatoms to monitor aquatic ecosystem change; charcoal as a proxy for fire and climate; Carbon/Nitrogen (C/N) ratio as an indicator for availability of organic matter; x-ray fluorescence (XRF) as a proxy for sediment geochemistry; and compare these datasets to pollen data (a proxy for vegetation change) from the same lake. Previous analysis of pollen and charcoal from the lake reveals more than 10 kyr, from 12,500 to 2500 years ago (12.5–2.5 ka), of climate-driven vegetation change in the absence of fire followed by a period of fire disturbance (ca. 2.5 ka to present) (Beck et al., 2018a; Fletcher et al., 2018a; Mariani and Fletcher, 2017). We use generalised additive models (GAMs) and their first derivatives to understand the type of response (direct or indirect) between multiproxy and multi-site datasets. GAMs are statistical models that can fit unevenly spaced time series data using a sum of smooth functions (Simpson, 2018a). Their first derivatives can be used to determine significant increases and decreases in GAM trends. Using this multiproxy dataset, we ask: (1) Is aquatic ecosystem change at Lake Vera driven by climate during the Holocene? (2) Do we observe similar responses in aquatic environments across the region? and (3) Does fire disturbance impact the aquatic ecosystem, and if so how?

2. Geography of site area

2.1. Study site

Lake Vera (42°16' 29'' S, 145°52'44'' E; 670 masl) is a small

moraine-bound lake formed in a glacial valley located on Frenchmans Cap, western Tasmania (Fig. 1) (Beck et al., 2018a; Fletcher et al., 2018a). The mean annual precipitation is ~1600 mm with a mean annual temperature of ~9 °C (Fletcher et al., 2018a). The lake is dystrophic, oligotrophic and acidic (Beck et al., 2018a). Lake Vera's bathymetry is asymmetric with a low lying sedge mat in the northeast end (Macphail, 1979; Peterson, 1966) and a steep gradient to a maximum depth of 48 m, meaning that the proportion of littoral habitat increases with increasing lake depth, while the proportion of open water increases with decreasing lake depth (Fig. 1e). Vegetation surrounding Lake Vera contains subalpine closed rainforest on the southeast facing slope of the valley dominated by *Andopetalum biglandulosum*, *Atherosperma moschatum*, *Eucryphia lucida*, *Nothofagus cunninghamii*, *Athrotaxis selaginoides*, and *Phyllocladus aspleniifolius*, with montane rainforest in the higher elevations dominated by *Athrotaxis cupressoides* and

Nothofagus gunnii (Fletcher et al., 2018a; Kitchener and Harris, 2013). The northwest facing slope contains *Eucalyptus* wet sclerophyll forest (*Eucalyptus* species overtop a rainforest understorey) with a *Gymnoschoenus sphaerocephalus* sedgelands on the lake's northeastern edge (Fletcher et al., 2018a; Macphail, 1979). The geology is mainly nutrient poor siliceous bedrock and glacial debris (Bradbury, 1986; Macphail, 1979).

2.2. Regional climate history

Lake Vera lies in the path of the zonal southern westerly winds (SWW), the dominant circulation system of the mid-to high-latitudes of the Southern Hemisphere (Garreaud, 2007). Seasonal to decadal-scale climatic variability, particularly rainfall, at Lake Vera is driven by variations in the latitudinal position and strength of the SWW, known as the Southern Annular Mode (SAM) (Fig. 1c)

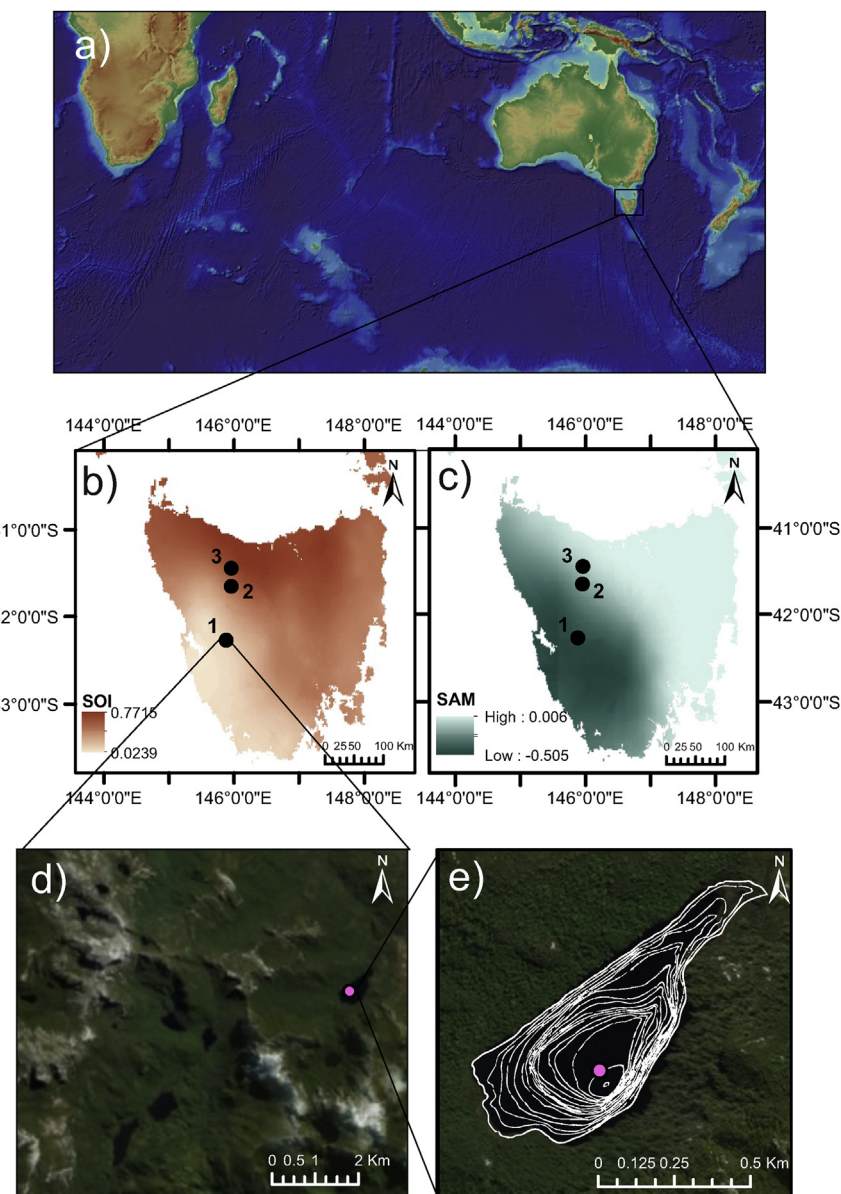


Fig. 1. a) Global digital elevation map of Australia and b&c) the location of (1) Lake Vera, (2) Dove Lake, and (3) Paddy's Lake in Tasmania (black dots) with precipitation correlation maps of b) the Southern Oscillation Index (Mariani and Fletcher, 2017), and c) the Southern Annular Mode (Mariani and Fletcher, 2017). Satellite images of the d) Lake Vera surrounding catchment; and e) Lake Vera coring location (pink dot) overlaid by the bathymetry determined by Peterson (1966), isobath intervals equal 10 feet (3.05 m). (For interpretation of the references to colour in this figure legend, the reader is referred to the Web version of this article.)

(Mariani and Fletcher, 2016, 2017). The period between ca. 12 to 5 ka was marked by a pattern of low frequency (multi-millennial) hydroclimate variability across the Southern Hemisphere resulting from changes in the strength and position of SWW (Fletcher and Moreno, 2012; Mariani and Fletcher, 2017; Saunders et al., 2018). In contrast, the period between ca. 5 kyr to present is marked by a shift toward higher frequency (centennial to millennial) hydroclimatic variability following the onset and amplification of the El Niño-Southern Oscillation (ENSO) (Barr et al., 2019; Mariani and Fletcher, 2017; Mariani et al., 2016). These climate transitions are responsible for important changes in terrestrial ecosystem dynamics across the Tasmanian landscape (Beck et al., 2017; Fletcher et al., 2014; Mariani et al., 2017; Stahle et al., 2017). For instance, the increased influence of burning during centennial-scale pulses of high frequency El Niño occurrence drove an increase in the importance of sclerophyllous vegetation (fire-adapted and fire-promoting vegetation) across the western Tasmanian landscape between ca. 6 to 2.5 ka (Barr et al., 2019; Beck et al., 2017; Fletcher et al., 2018b; Hopf et al., 2000; Mariani et al., 2017).

3. Methods

3.1. Coring and chronology

Two cores were collected from Lake Vera to create the composite record. In 2011 a sediment-water interface core of 105 cm in length (TAS1108 SC1) was collected from the deepest point in Lake Vera using the Universal coring system (Aquatic Research Instruments, 2018). In 2015 a long continuous core of 5.34 m (TAS1508 N1) was collected from the same deep basin using a Nesje system (Nesje, 1992). Charcoal counts and XRF data were used to tie cores TAS1108 SC1 and TAS1508 N1 into a composite record. TAS1108 SC1 data were binned to 0.1 cm depths in R v. 3.5.1 (R Development Core Team, 2014) to match the sample depths of TAS1508 N1. An r^2 was determined between the TAS1508 N1 INC/COH data and the TAS1108 SC1 INC/COH binned data for three key tie points to determine the most robust tie point: 1) TAS1508 N1 72.3–74.1 cm and TAS1108 SC1 89.2–91.0 cm, 2) TAS1508 N1 85.0–86.4 cm and TAS1108 SC1 97.5–98.9 cm, and 3) TAS1508 N1 91.6–94.0 cm and TAS1108 SC1 100.8–103.2 cm.

Radiometric dating analysis was performed at the Australian Nuclear Science and Technology Organisation (ANSTO) (five ^{210}Pb samples from TAS1108 SC1), the National Ocean Sciences Accelerator Mass Spectrometry (NOSAMS) (four radiocarbon bulk sediment samples from TAS1108 SC1) and DirectAMS (16 radiocarbon macrofossil samples from TAS1501 N1) (Table 1). Radiocarbon dates were calibrated with the Southern Hemisphere calibration curve - SHCal13 (Hogg et al., 2013). The Constant Initial Concentration (CIC) model based on ^{210}Pb ages (Appleby, 2001) was chosen because of presumed constant sedimentation due to the deep anoxic nature of the lake (Beck et al., 2018a). A Bayesian age-depth model was developed in R using the Bacon v. 2.2 package (Blaauw and Christen, 2013) for the composite core (TAS1108 SC1 and TAS1508 N1).

3.2. Geochemical analysis

Analyses of percent organic Carbon (%C) and Nitrogen (%N), was performed on a Carlo Erba Elemental Analyser (CHNS-O EA1108 - Italy) for TAS1108 SC1 at the Elemental Isotope Laboratories, Wilfrid Laurier University, and a EuroVector EuroEA Elemental Analyser for TAS1508 N1 at the University of Adelaide. Samples were analysed every 0.5 cm for TAS1108 SC1 and 5 cm intervals for TAS1508 N1 and calibrated to international standards (IAEA N1, N2, NO3, C6, and C7; USGS 24, 25, 32, 40, and 41; and NBS 22). The C/N ratio was calculated from the %C and %N.

Geochemical data were obtained using the non-destructive Itrax micro X-ray fluorescence (XRF) core scanner at ANSTO at a resolution of 0.2 mm for TAS1108 SC1 and 1.0 mm for TAS1508 N1 using a molybdenum (Mo) tube set by a voltage of 30 kV, a current of 45 mA, and a dwell time of 10 s. The elemental dataset was normalised by the Mo Incoherent/Coherent ratio (INC/COH), a standard technique to remove the effects of water content (Croudace and Rothwell, 2015). Iron (Fe) is used here as an indicator of iron richness (Croudace and Rothwell, 2015) and the INC/COH ratio is used as an indicator of shifts in organic and inorganic matter (Croudace and Rothwell, 2015). A Principal Component Analysis (PCA) was performed in R using the vegan package v. 2.5-4 (Oksanen et al., 2019) on the XRF normalised data using a Hellinger transformation. The number of significant axes was determined using a broken stick model in the R package vegan. A square root transformation was performed before the ordination analysis to normalise the data to combat arch effects.

3.3. Pollen and charcoal

Pollen was processed using 0.5 cc of sediment by standard methods (Faegri and Iversen, 1989) and sampled at various intervals depending on depositional rates of the cores. A minimum of 300 terrestrial pollen grains were identified per sample using a bright field objective at 400 \times magnification. Percentages were determined using the terrestrial pollen sum. Aquatic and spore pollen percentages were calculated from the supersum including all pollen and spores. *Blechnum* spp., *Dicksonia antarctica*, *Hypolepis* spp., *Microsorum* spp., and *Polystichum proliferum* were summed to create a total percent ferns curve and *Baeckea* spp., *Eucalyptus* spp., *Leptospermum* spp., *Melaleuca* spp., and other Myrtaceae spp. were summed to create a percent sclerophyllous taxa curve. A PCA was performed in R using the vegan package on the normalised terrestrial pollen percent taxa with Hellinger transformation, and a broken stick model was applied to determine the number of significant axes. A square root transformation was performed before the ordination analysis to normalise the data to combat arch effects.

Macroscopic charcoal was processed at 0.5 cm intervals for TAS1108 SC1 and 2.0 cm intervals for TAS1508 N1 according to standard protocols (Whitlock and Larsen, 2001). A volume of 1.5 mL (TAS1108 SC1) to 1.25 mL (TAS1508 N1) of sediment was placed in household bleach for at least seven days then sieved through 250 μm and 125 μm meshes and enumerated under a stereomicroscope at 10–20 \times magnification. Composite charcoal accumulation rate (CHAR_{acc}) was calculated from summed TAS1108 SC1 and TAS1508 N1 macroscopic charcoal counts.

3.4. Diatoms

Diatom remains in sediment archives can provide an array of information on past environments where instrumental data are not available. The autecology of Australian diatoms is limited, even more so in Tasmania where there is a high degree of endemism (John, 2018). Many diatom taxa in Tasmania have more species in common with New Zealand and sub-Antarctic islands than mainland Australia. Where possible species ecological preferences were determined using Tasmanian sources (i.e. John, 2018; Kilroy et al., 2003; Kocielek et al., 2004; Sabbe et al., 2001; Saunders et al., 2009; Saunders et al., 2015; Vanhoutte et al., 2004; Vyverman et al., 1995; Vyverman et al., 1996); however, in some instances species ecology was inferred from other regions i.e. New Zealand, mainland Australia, Antarctica, and other temperate regions (Foged, 1978; Gell, 1999; John, 1983, 2016; Spaulding et al., 2010, 2019). While diatoms are sensitive to numerous environmental drivers, in the freshwater systems of Tasmania, a west to east

Table 1

Radiocarbon results for Lake Vera (TAS1108 SC1 & TAS1508 N1), including the laboratory identification number, core name, sample depth (cm), sample type, the pMC and error (1σ), the radiocarbon age (BP) and error, and $\delta^{13}\text{C}$ (per mil).

Lab code	Core	Depth (cm)	Sample Type	pMC	Error (1σ)	Age	Age Error	$\delta^{13}\text{C}$	
1	OS-92421	TAS1108 SC1	23–23.5	bulk organic sediment	0.9222	0.0028	650	25	-27.72
2	OS-92422	TAS1108 SC1	50–50.5	bulk organic sediment	0.8543	0.0034	1260	30	-27.6
3	OS-92423	TAS1108 SC1	81–81.5	bulk organic sediment	0.7758	0.0029	2040	30	-27.55
4	OS-89128	TAS1108 SC1	103.5–104	bulk organic sediment	0.7423	0.0025	2390	25	-27.15
5	D-AMS 015676	TAS1501 N1	114–114.5	plant macrofossil	77.38	0.33	2060	34	-32.9
6	D-AMS 015678	TAS1501 N1	131–131.5	plant macrofossil	76.32	0.34	2171	36	-27.7
7	D-AMS 015682	TAS1501 N1	185–185.5	plant macrofossil	59.65	0.67	4150	90	-29.2
8	D-AMS 017892	TAS1501 N1	195–195.5	plant macrofossil	68.32	0.24	3060	28	NA
9	D-AMS 015680	TAS1501 N1	238.5–239	plant macrofossil	61.73	0.3	3875	39	-21
10	D-AMS 016846	TAS1501 N1	298–298.5	plant macrofossil	57.1	0.17	4501	24	-30.5
11	D-AMS 015683	TAS1501 N1	309.5–310	plant macrofossil	50.66	0.25	5463	40	-32.5
12	D-AMS 017893	TAS1501 N1	358.5–359	plant macrofossil	43.41	0.2	6703	37	NA
13	D-AMS 016847	TAS1501 N1	359–360	plant macrofossil	42.28	0.16	6915	30	-30.8
14	D-AMS 017894	TAS1501 N1	383.5–384	plant macrofossil	46.26	0.31	6193	54	NA
15	D-AMS 016852	TAS1501 N1	399–399.5	plant macrofossil	48.07	0.15	5884	25	-24.4
16	D-AMS 016848	TAS1501 N1	419.5–420	plant macrofossil	46.92	0.23	6079	39	-19.4
17	D-AMS 016849	TAS1501 N1	448–448.5	plant macrofossil	43.79	0.15	6633	28	-29.5
18	D-AMS 016850	TAS1501 N1	462–462.5	plant macrofossil	42.07	0.14	6955	27	-27.6
19	D-AMS 016851	TAS1501 N1	476–476.5	plant macrofossil	41.15	0.14	7133	27	-30
20	D-AMS 017895	TAS1501 N1	525.5–526	plant macrofossil	36.6	0.2	8074	44	NA

gradient across the island exerts the greatest influence over species occurrence and composition. Western lakes are acidic, humic with ionic compositions similar to sea water, while eastern lakes are clear (ultra)oligotrophic with higher pH, alkalinity and ionic compositions closer to the world average of fresh water (Vyverman et al., 1995, 1996).

Diatom analysis was performed using 0.5 cc of sediment by standard methods (Battarbee, 1986; Bradbury, 1986). Sample intervals varied depending on depositional rates of the cores. Known concentrations of residues were mounted using Naphrax® and a minimum of 300 diatom valves were identified per slide using an oil immersion DIC objective at 1000 \times magnification. Diatom concentration was determined using known sediment concentrations and dilutions on slides and identified along transects of defined length. The total *Aulacoseira* spp. abundance was determined using the sum of *Aulacoseira alpigena*, *Aulacoseira crassipunctata*, *Aulacoseira crenulata*, *Aulacoseira distans*, *Aulacoseira pfaffiana*, and *Aulacoseira valida*. The planktonic:benthic ratio was calculated using the sum of planktonic taxa divided by benthic taxa and excludes tytoplanktonic taxa (see Supplementary Data Table S4). Diatom taxonomic nomenclature was defined using Algaebase (<http://www.algaebase.org/>) and all diatom taxa and authority names are included in the Supplementary Data (Table S4). A PCA was performed on diatom percent taxa with a Hellinger transformation and a broken stick model was applied to determine the number of significant axes using the vegan package in R.

3.5. Generalised additive models and derivatives

Generalised additive models were used to estimate trends of unevenly spaced time series data using smooth functions. The GAMs were fitted to ordination axes scores for diatoms, pollen, XRF data and other important species and geochemical data. GAMs are semiparametric regression models that fit a response variable to co-variates using a sum of smooth functions (Hastie and Tibshirani, 1990; Simpson, 2018a; Simpson and Anderson, 2009; Yee and Mitchell, 1991). GAMs were fitted with the residual maximum likelihood (REML) method to penalise overfitting trends (Wood, 2011, 2016) using the mgcv v. 1.8-25 package in R (Wood, 2016). A Gaussian distribution with an identity link was used to model the time series data with one covariate to account for age uncertainty in the models (Simpson, 2018a). Base functions (k) were selected

depending on the number of samples in the time series being modelled to achieve the best model fit (see Table S3 in Supplementary Data for more details). The first derivative functions of these GAMs were identified and used to determine significant trends in the time series data (Bennion et al., 2015; Mariani and Fletcher, 2017; Simpson, 2018a). The derivatives and 95% confidence interval, determined by point-wise simulations ($n = 10,000$), were calculated using the R package gratia v. 0.1-4 (Simpson, 2018b), where trends that deviated from 0 (no trend) indicate periods of significance. GAMs and derivatives were not determined for some time series data due to poor fit (i.e. CHAR_{acc}). Significant shifts determined by the first derivatives provide a temporal anchor for important shifts in the time series data. Thus, changes in the PCA supported by the statistical analyses of the GAM first derivatives were used to interpret important shifts in the palaeoecological record at Lake Vera. Statistical results of fitted GAMs can be found in the Supplementary Data (Table S3).

4. Results

4.1. Coring and chronology

The composite sediment core did not reach the basal sediments. The oldest radiocarbon date of 8074 ± 44 ^{14}C years was at 526 cm and unsupported ^{210}Pb reached background at 5 cm (Fig. 2). Table 1 summarises radiocarbon dating results for TAS1108 SC1 and TAS1508 N1. For details on ^{210}Pb results see Supplementary Data (Table S1). The age model shows reasonably linear accumulation for the composite core (TAS1108 SC1 & TAS1508 N1) with a mean accumulation rate of 20 yr/cm (Fig. 2) and a slight change in sedimentation rate between the two cores due to compaction of the surface core TAS1108 SC1. Charcoal and r^2 of XRF data were used to tie TAS1108 SC1 and TAS1508 N1 into a composite record. The r^2 values for the three key INC/COH tie points were 1) $r^2 = 0.31$, 2) $r^2 = 0.22$, and 3) $r^2 = 0.82$. These results determined the most robust tie point occurs at 102 cm for TAS1108 SC1 and 92 cm for TAS1508 N1 (Fig. 3).

4.2. Geochemical analysis

The XRF dataset has an average resolution of ca. 1 yr. The XRF PCA axis 1 is the only significant axis with an explained variance of

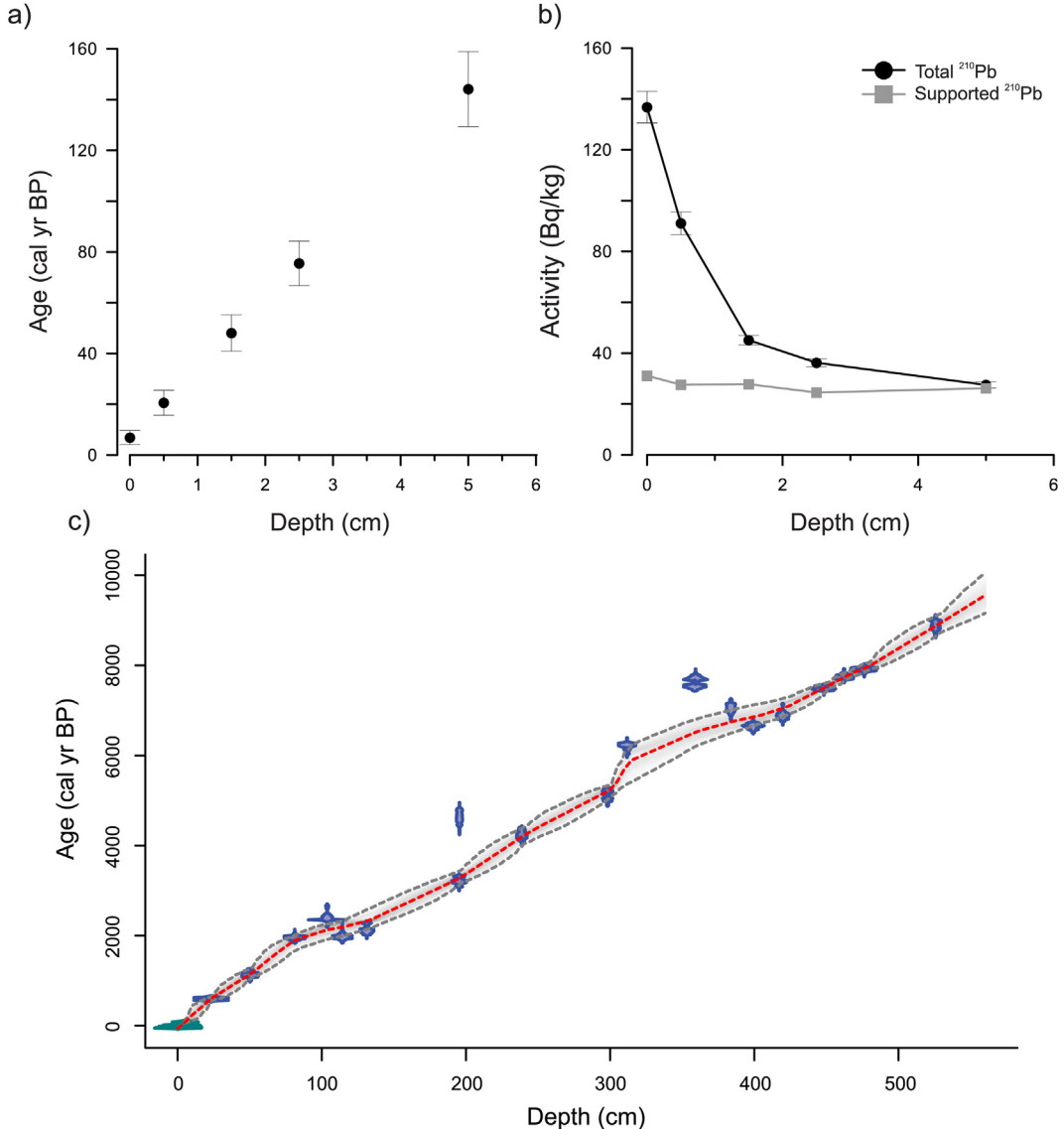


Fig. 2. Lake Vera age model. a) ^{210}Pb CIC age-depth model; b) ^{210}Pb activity of total (black) and supported (grey) ^{210}Pb with errors by depth (cm); and c) Bacon age model with probability distribution of the radiocarbon ages (blue) and age probability of ^{210}Pb dates (green). The 1000 iterations of potential depth ages (Bayesian statistic, black dotted lines) are shown with the 95% confidence interval (grey dotted lines) and the age-depth model of this study (red dotted line). (For interpretation of the references to colour in this figure legend, the reader is referred to the Web version of this article.)

66.3%. XRF PCA 1 shows a strong positive association with Fe, K, Rb, Co, and Ti and a negative association with INC/COH, Br, Cu, and Ca (Supplementary Data Table S2 and Fig. S3). XRF PCA axis 1 GAM declines from ca. 9.2 to 7.7 ka, followed by an increase to ca. 6.8 ka with a decline to a minimum at ca. 6.5 ka. The axis scores show a declining trend to ca. 2.5 ka followed by an increase to present. Five major peaks occur at ca. 5.8, 4.5, 2.3, 1.5, and 0.8 ka (Fig. 4c). INC/COH shows a slight increase across the time series, with low values at ca. 9.1, 8.1, 6.6, 5.7, 4.4, 4.2, 3.8, 2.3, 2.0, 1.5, 1.4, 0.8, and 0.4 ka and peaks at ca. 6.2, 4.0, 3.4, 1.8 ka and present (Fig. 4a). The Fe GAM reveals a general declining trend from ca. 9.2 to 7.8 ka followed by an increase to a peak at ca. 7.4 ka and again at ca. 6.8 ka. Values decline until ca. 2.5 ka followed by an increasing trend to present (Fig. 4b). Low values occur at ca. 7.8, 6.5, 6.2, 4.0, and 2.5 ka and high values occur at ca. 9.0, 6.9, 5.9, 4.5, 1.4, 0.8 ka and present. The C/N results have an average resolution of ca. 31 yrs. The C/N ratio GAM shows stable values around 26.5% from ca. 9.2 to 7.5 ka, followed by an increase to ca. 7.0 ka and decline again to ca. 5.5 ka. Values

peak at ca. 4.3 ka (36.6%) and 2.3 ka (38.9%), followed by an increase at ca. 0.8 and 0.5 ka and a decline to present (Fig. 4d). The XRF PCA biplot and an extended stratigraphy can be found in the Supplementary Data (Figs. S3 and S4).

4.3. Pollen and charcoal

Pollen samples have an average resolution of ca. 48 yrs. The pollen PCA has two significant axes, axis 1 has an explained variance of 37.2% and axis 2 has an explained variance of 15.3%. Important transitions in the diatom stratigraphy at ca. 6.5, 4.0, 2.2, & 0.9 ka (Fig. 6) were projected onto the pollen stratigraphy (Fig. 5). PCA axis 1 has a strong negative association with *Nothofagus cunninghamii*, *Nothofagus gunnii*, *Phyllocladus aspleniifolius*, and *Rhamnaceae* and a strong positive association with *Lagarostrobus franklinii*, *Leptospermum/Baeckea*, *Melaleuca* spp., and *Microcachrys* spp. (Supplementary Data Table S2). The pollen PCA biplot can be found in the Supplementary Data (Fig. S2). CHAR_{acc} has an average

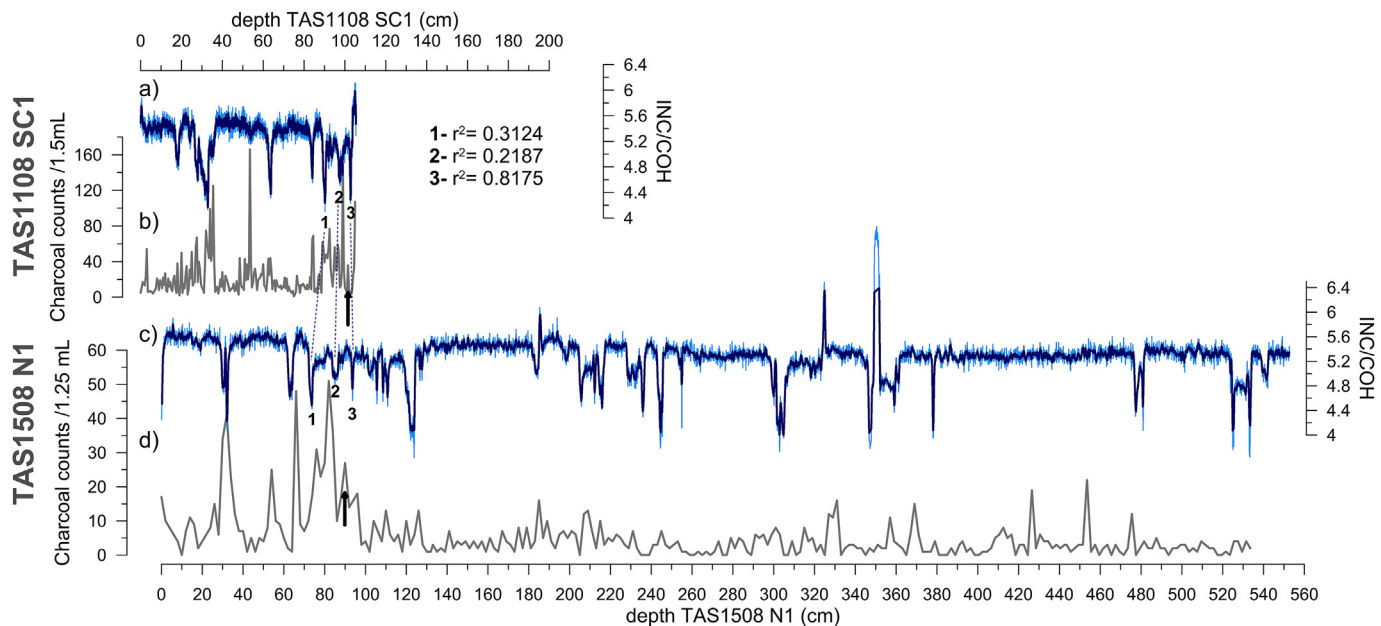


Fig. 3. Composite core tie points from TAS1108 SC1 a) XRF INC/COH ratio (light blue) with a 5-point moving average (dark blue) and b) raw charcoal counts by depth compared to TAS1508 N1 c) XRF INC/COH ratio (light blue) with a 5-point moving average (dark blue) and d) raw charcoal counts. The black arrows indicate the tie point depths between the core charcoal counts and blue dotted lines indicate tie points between cores XRF INC/COH ratios. R^2 values for the three INC/COH tie points are (1) $r^2 = 0.31$, (2) $r^2 = 0.22$, and (3) $r^2 = 0.82$. (For interpretation of the references to colour in this figure legend, the reader is referred to the Web version of this article.)

resolution of ca. 22 yrs and shows very low values from ca. 9.2 to 2.6 ka. At ca. 2.6 ka values increase, followed by a further increase to a maximum at ca. 2.3 ka with peaks in the remainder of the record at ca. 2.1, 2.0, 1.9, 1.4, 1.2, 0.9, 0.8, and 0.7 ka (Fig. 4v and 8g).

Fern pollen declines from the start of the record to ca. 4.6 ka, followed by an increase to ca. 3.7 ka and decline again to ca. 2.0 ka. They rapidly increase to ca. 0.4 ka followed by a short decline to present (Fig. 4e). Sclerophyllous taxa have low abundances until ca. 3.4 ka, followed by an increasing trend to present (Fig. 4f). *Lagarostrobus franklinii* has low abundance from ca. 9.2 to 5.2 ka then rapidly increases to maximum abundance at ca. 3.0 ka followed by a gradual decline to present (Fig. 4g). *Isoëtes* shows a general decline throughout the record with peaks at ca. 6.6 and 2.5 ka (Fig. 4h). *Nothofagus gunnii* increases to maximum abundance at ca. 6.5 ka, then declines to present (Fig. 4i). *Phyllocladus aspleniifolius* increases to maximum abundance at ca. 5.0 ka, followed by a declining trend to ca. 1.2 ka and a general increasing trend to present. Peak abundances occur at ca. 8.3, 6.7, 5.0, and 2.7 ka (Fig. 4j). PCA axis 1 has low values with peaks at ca. 7.0 and 5.7 ka followed by an increasing trend from ca. 5.0 to 1.3 ka, a decline to ca. 0.3 ka, and increase again to present (Fig. 4k). Rainforest pollen increases from ca. 9.2 to 8.1 ka with high stable values to ca. 5.1 ka, followed by a decline to ca. 1.2 ka and increase to present (Fig. 7e).

4.4. Diatoms

Diatoms show good preservation throughout the composite record with ~318 species identified at an average resolution of ca. 68 yrs (Fig. 6). The diatom community at Lake Vera is dominated by rare taxa, only 31 taxa occur with a maximum abundance above 3%. Two PCA axes were significant, where diatom PCA axis 1 has an explained variance of 24.7% and is positively associated with *Dis-costella stelligera*, *Achnanthidium minutissimum*, and *Fragilaria capucina* and is negatively associated with *Eunotia diodon*, *Staur-iforma exiguaformis*, *Eunotia implicata*, *Aulacoseira distans*, and *Frustulia elongatissima*. PCA axis 2 has an explained variance of

12.2% with a strong positive association with *A. minutissimum*, *Achnanthes subexigua*, *Brachysira styriaca*, and *Brachysira microcephala* and a negative association with *D. stelligera*, *E. diodon*, *Gomphonema multiforme*, *Eunotia incisa* and *F. elongatissima*. The diatom PCA biplot and PCA species scores can be found in the Supplementary Data (Fig. S1 & Table S2).

Important transitions in the diatom stratigraphy occur at ca. 6.5, 4.0, 2.3, & 0.9 ka (Fig. 6) and were determined using temporal transitions identified by shifts in PCA axes 1 & 2 and diatom assemblage data with assistance from significant shifts in the GAMs. *Aulacoseira* spp. increases to maximum abundance from ca. 9.2 to 6.6 ka followed by a decline to ca. 1.6 ka and low abundance to present (Fig. 4l). *S. exiguaformis* increases to maximum abundance from ca. 9.2 to 6.7 ka, followed by a decline to ca. 3.2 ka and slight increase to peak at ca. 0.7 ka (Fig. 4m). *E. diodon* declines from ca. 9.2 to 8.2 ka, followed by an increase to maximum abundance at ca. 6.0 ka. Abundances then decline to ca. 1.7 ka followed by an increase to present (Fig. 4n). *F. elongatissima* increases in abundance from ca. 9.2 to 5.5 ka followed by a decline to ca. 1.7 ka and a rapid increase to present (Fig. 4o). *A. subexigua* declines from ca. 8.6 to ca. 5.7 ka and increase to ca. 4.5 ka. Abundances decline and plateau from ca. 3.6 to 2.4 ka, followed by an increase to maximum abundance at ca. 1.5 ka and rapid decline to 0.5 ka followed by an increase to present (Fig. 4p). *A. minutissimum* shows a gradual decline from ca. 9.2 to 5.0 ka, followed by an increase to ca. 4.0 ka then a rapid increase to maximum abundance at ca. 1.6 ka and a decline again to present (Fig. 4q). *D. stelligera* decreases from ca. 9.2 to 8.8 ka, plateaus, and then decreases again to ca. 6.4 ka. There is a slight increase in abundance to ca. 5.8 ka followed by a rapid increase to maximum abundance at ca. 3.5 ka. For the remainder of the record, *D. stelligera* dominates with variable abundance. Peak abundances occur at ca. 3.5, 2.0, and 0.7 ka, followed by a decline to present (Fig. 4r). The total diatom valves show a slight decline from ca. 9.2 to 5.8 ka followed by an increase to ca. 3.4 ka and from ca. 2.6 to 1.7 ka. From ca. 1.4 to 0.8 ka the total diatom valves decline with low concentration to present (Fig. 4s). PCA axis 1 shows a declining

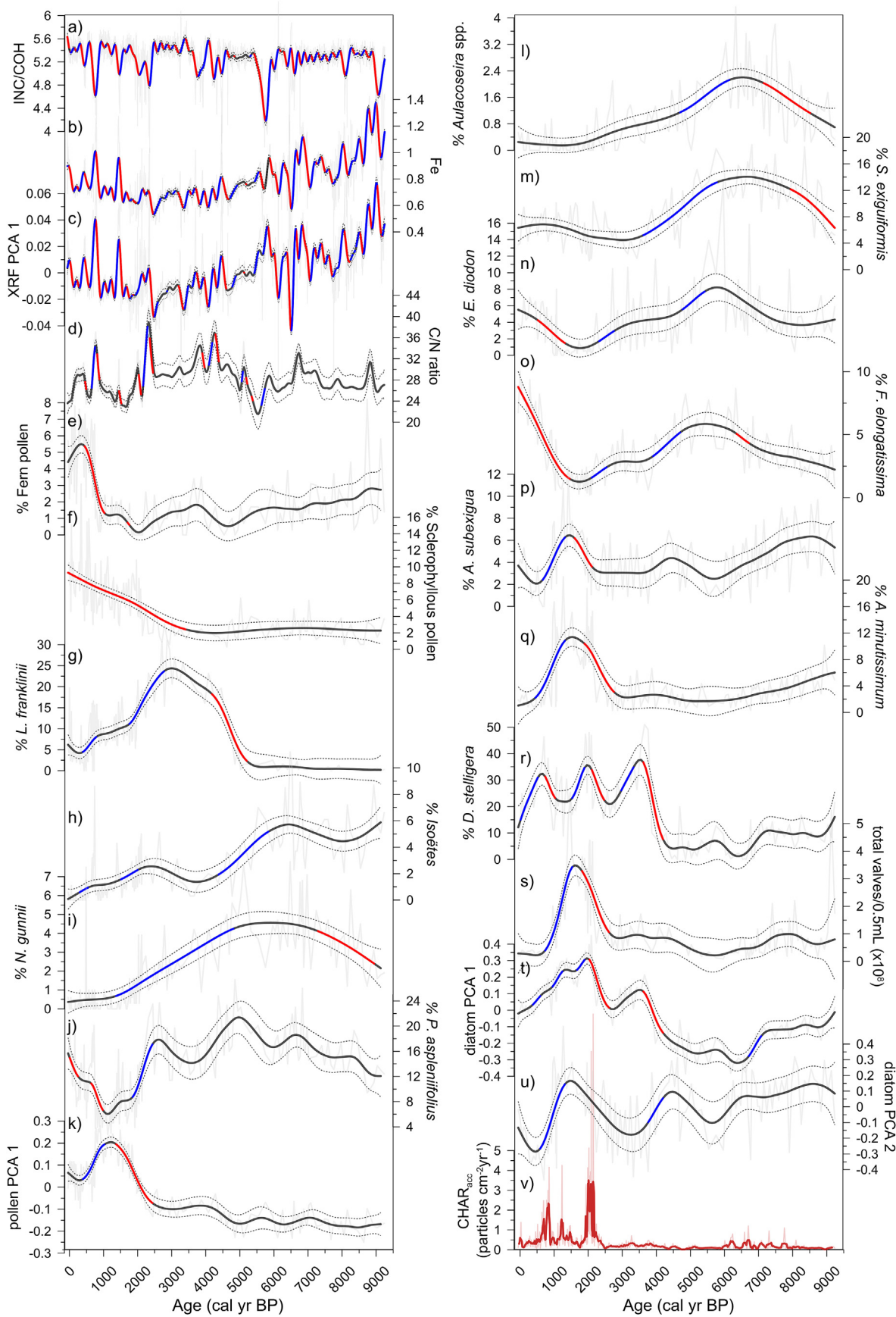


Fig. 4. Lake Vera proxy data fit with GAMs (black) and associated confidence intervals (grey dotted lines). On the left: a) XRF INC/COH; b) XRF Fe; c) XRF PCA axis 1; d) C/N ratio; pollen percentages of e) Ferns; f) Sclerophyllous taxa; g) *Lagarostrobus franklinii*; h) *Isoëtes*; i) *Nothofagus gunnii*; j) *Phyllocladus asplenifolius*; and k) pollen PCA 1. On the right

trend from ca. 9.2 to 6.4 ka followed by an increase to 2.0 ka with peaks at ca. 8.4, 5.6, and 3.5 ka. Scores then decline to present (Fig. 4t). PCA axis 2 shows a general decline from ca. 9.2 to 5.7 ka followed by an increase to ca. 4.6 ka and decline again to ca. 3.3 ka. Values increase to a maximum at ca. 1.5 ka followed by decrease to lowest values at ca. 0.5 ka with an increase again to present (Fig. 4u).

4.5. Generalised additive models and derivatives

Statistical results for the GAM fits can be found in the Supplementary Data (Table S3). Some GAMs did not have good fit to the time series data because either (1) abrupt shifts in the dataset could not be modelled due to GAMs use of smooth functions (i.e. CHAR-acc), or (2) time series that have the appearance of good fit did not show good statistical outputs due a high number of data points (i.e. XRF data). Results of the first derivatives are summarised in Fig. 4 where red shading indicates significant increases and blue shading significant decreases in the fitted GAMs. Full first derivative results can be found in the Supplementary Data (Figs. S5, S6, and S7).

5. Discussion

5.1. Palaeoenvironment at Lake Vera

5.1.1. Landscape and lake development (ca. 9.2 to 4 ka)

Our data indicate that the long-term evolution of the terrestrial and aquatic environments at Lake Vera tracks regional SWW-driven hydroclimatic shifts during the early to mid-Holocene (ca. 9.2 to 3.8 ka). During this period, the trends in rainforest compositional change (increasing *Phyllocladus aspleniifolius* and *Nothofagus gunnii* pollen; Fig. 4i and j) at Lake Vera is consistent with regional moisture-driven western Tasmanian charcoal trends (Fig. 7a) (Fletcher and Moreno, 2012; Mariani and Fletcher, 2017). Within the lake, from ca. 9.2 to 3.8 ka, low diatom productivity and abundant tychoplanktonic pioneer taxa (*S. exiguum*, *Staurosira construens*, *Staurosira venter*, *Staurosira pinnata*, and *Tabellaria flocculosa*) (Augustinus et al., 2012; Gell and Reid, 2014; Law et al., 2015; Saunders et al., 2013) and other small benthic taxa (*Eunotia diodon*, *Eunotia implicata*, and *Frustulia elongatissima*) (Figs. 4 and 6) indicate Lake Vera was relatively full. The increase in benthic over planktonic diatom taxa under full lake conditions (Fig. 6) is consistent with an increase in the available littoral habitat dictated by the bathymetry of Lake Vera (Fig. 1). The tychoplanktonic and pioneer nature of the diatom assemblage also indicates a turbulent and rapidly changing environment (Augustinus et al., 2012; Law et al., 2015; Saunders et al., 2013), consistent with high rainfall and terrigenous deposition from the surrounding catchment (Fig. 4a–d).

Peak regional moisture in western Tasmania between ca. 7 to 4 ka (Fig. 7a) is coeval with increasing abundance of heavy siliceous diatoms, *Aulacoseira* spp. and *Brevicula arenii* (Figs. 4l & 6), species that require strong mixing provided by turbulent waters (Gell and Reid, 2014; Saros and Anderson, 2015; Saunders et al., 2009; Tibby et al., 2012). A strengthening of the SWW over Tasmania from ca. 9 to 6.5 ka resulted in increased rainfall and windy conditions in the west of the island (Fletcher et al., 2015; Fletcher and Moreno, 2011, 2012; Rees et al., 2015; Saunders et al., 2018), increasing lake levels and turbulent waters. Further, the formation of an extensive littoral

zone under turbulent and oligotrophic full lake conditions is supported by the high abundance of *Isoëtes* between ca. 9.2 and 6.5 ka, a plant macrophyte tolerant of low light, oligotrophic environments, and wave erosion (Fig. 4h) (Beck et al., 2017; Rørslett and Brettum, 1989).

The continued development of a rainforest-dominant catchment in response to increased moisture and low to absent fire activity is reflected in the diatom flora with an increase in taxa tolerant of acidic and dystrophic lake water conditions (e.g. *B. arenii*, *E. diodon*, *E. implicata*, and *F. elongatissima*) at ca. 6.5 ka (John, 2018; Sherman et al., 1998; Steinberg, 2003; van Dam et al., 1981). Rainforest on the nutrient deficient bedrock of western Tasmania occurs on peat (Bowman and Jackson, 1981). Indeed, low pH and dystrophy are ubiquitous limnological characteristics in this landscape, due to the predominance of blanket peats (Brown et al., 1982; Buckney and Tyler, 1973; Steane and Tyler, 1982; Tyler, 1974). Thus, we hypothesise that the uninterrupted rainforest development during the early to mid-Holocene resulted in an accumulation of the underlying peat layer within the catchment, thus increasing the amount of terrestrial humic acids delivered into the lake and resulting in the development of acidic and dystrophic lake waters (Fig. 4). Moreover, this inference is consistent with increased terrestrial organic indicators (C/N, Fe, Fig. 4b and d) coeval with the diatom trend toward low pH and high dystrophy (Figs. 4 and 6).

5.1.2. Regional drying ca. 4 ka

A shift toward a more variable and overall drier hydroclimate after ca. 5 ka (Fletcher et al., 2015; Mariani and Fletcher, 2017) is marked by an increase in fire across western Tasmania, with a marked and sustained increase in regional burning occurring at ca. 4 ka (Fig. 7a). This shift in regional hydroclimate is coeval with changes in the terrestrial and aquatic environment at Lake Vera (Fig. 7). A shift from high relative importance of rainforest taxa, such as *N. gunnii* and *P. aspleniifolius* (Fig. 4i and j), to dominant *L. franklinii* (Fig. 4g), a rainforest species with a reproductive cycle triggered by drought stress (Fletcher, 2015), indicates a clear response of the rainforest to regional climate change (Beck et al., 2017; Fletcher, 2015; Mariani and Fletcher, 2017). Therefore, lower rainfall and a resultant decline in littoral habitat under lower lake levels is indicated by (1) a reduction in the aquatic macrophyte, *Isoëtes* (Fig. 4h), (2) an increase in the planktonic:benthic diatom ratio (Fig. 6), and (3) a dominance of planktonic *Discostella stelligera* from ca. 3.8 ka (Fig. 4r).

5.1.3. Onset of fire ca. 2.6 ka to present

Our data indicate an onset of local fire activity between ca. 2.6 to 0.7 ka, much later than regional fire trends (ca. 4 ka) but consistent with a drying and more variable climate (Fig. 7a) (Mariani and Fletcher, 2017; Mariani et al., 2016). This later response at Lake Vera is likely due to the heavily rainforest catchment, trapping moisture and resisting burning (Jackson, 1968). However, overtime, continued drying allows Lake Vera to become more vulnerable to fire due to moisture loss and increasing sclerophyllous vegetation. The anomalous diatom assemblage (Figs. 4 and 6) between ca. 2.3 to 0.9 ka is likely caused by fire, change in vegetation, and the deposition of ash and terrestrial matter (both organic and inorganic) (Fig. 8b and d).

Repeated fire disturbance within the Lake Vera catchment drove an increase in light-demanding ferns, fire adapted and promoted sclerophyll taxa (Fig. 4e and f, and 8e), and an increase in the

diatom percentages for: l) *Aulacoseira* spp.; m) *Stauroforma exiguum*; n) *Eunotia diodon*; o) *Frustulia elongatissima*; p) *Achnanthes subexigua*; q) *Achnanthidium minutissimum*; r) *Discostella stelligera*; s) total diatom valves per mL ($\times 10^8$); t) diatom PCA 1 axis and u) diatom PCA axis 2. Red shaded areas indicate significant increasing trends and blue shaded areas indicate significant decreasing trends determined by the first derivatives. v) Macroscopic charcoal accumulation (particles $\text{cm}^{-2} \text{yr}^{-1}$) (light red) fit with a weighted average (window width = 5) (red). (For interpretation of the references to colour in this figure legend, the reader is referred to the Web version of this article.)

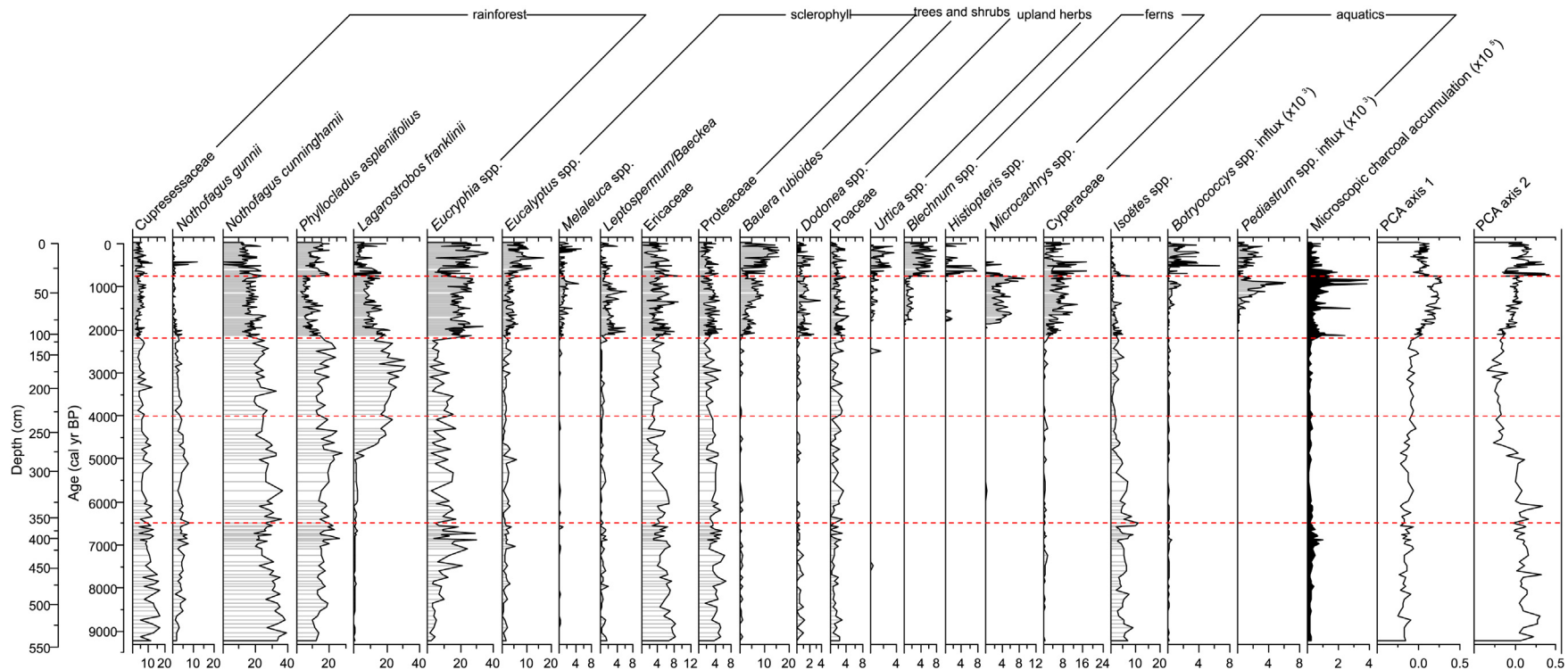


Fig. 5. Lake Vera pollen stratigraphy of most important pollen taxa presented as percentage composition. *Botryococcus* and *Pediastrum* spp. are shown as influx and microscopic charcoal as an accumulation rate. The PCA axes estimate trends in the terrestrial pollen percentage data, with axis 1 explaining 37.2% of the variance and axis 2 explaining 15.3% of the variance. Red dashed lines indicate transitions in the diatoms determined by shifts in PCA axes and GAM results of the diatoms. (For interpretation of the references to colour in this figure legend, the reader is referred to the Web version of this article.)

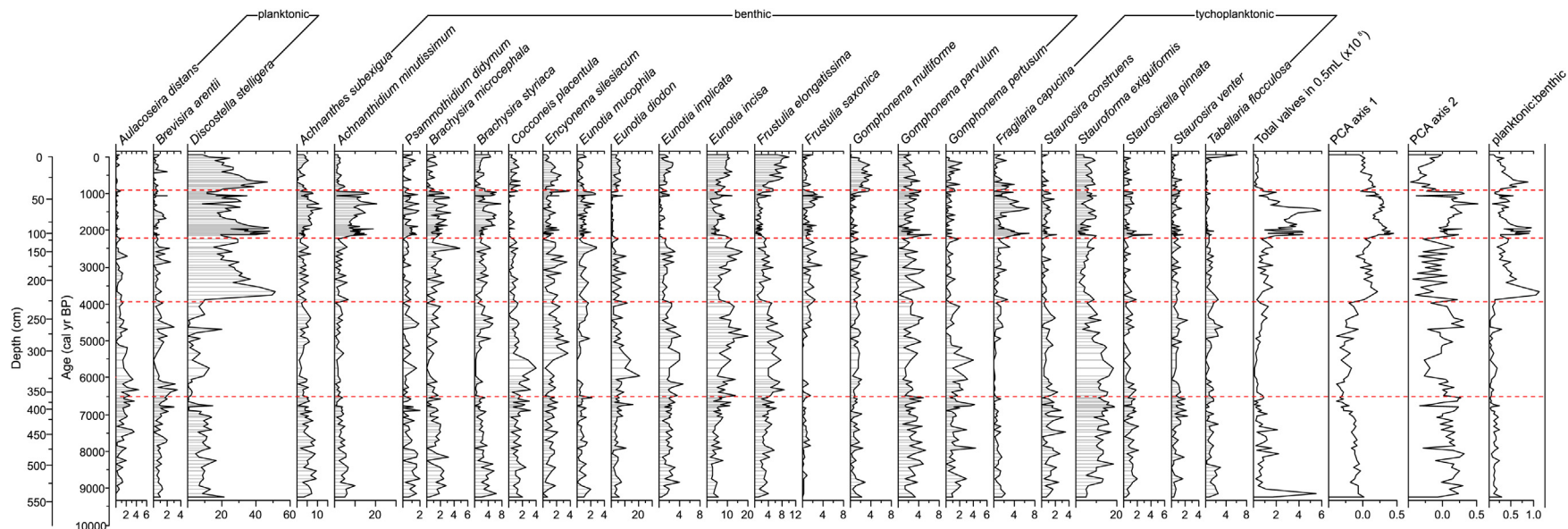


Fig. 6. Lake Vera diatom stratigraphy of the most abundant diatom species presented as percent relative abundance. The PCA axes estimate trends in the diatom percentage data, with axis 1 explaining 24.7% of the variance and axis 2 explaining 12.2% of the variance. Planktonic:benthic ratio estimate trends in the sum of planktonic to benthic taxa (excluding tychoplanktonic taxa). Red dashed lines indicate transitions in the diatom data determined by shifts in PCA axes and GAM results. (For interpretation of the references to colour in this figure legend, the reader is referred to the Web version of this article.)

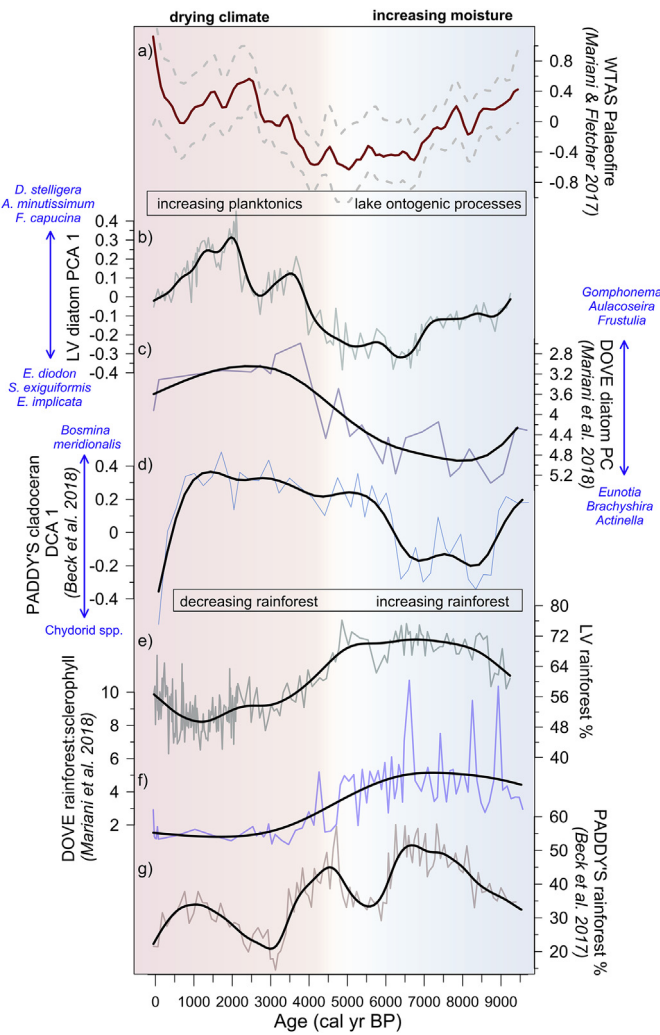


Fig. 7. Summary plot of western Tasmanian terrestrial-aquatic proxy data during the Holocene. a) western Tasmanian regional composite charcoal z-scores from 13 charcoal records (red) with upper and lower boundaries (grey dashed lines) (Mariani and Fletcher, 2017); b) Lake Vera (LV) diatom PCA axis 1 with fitted GAM; c) Dove Lake diatom principle curve in descending order with fitted GAM (Mariani et al., 2018); d) Paddy's Lake cladoceran Detrended Component Analysis (DCA) axis 1 with fitted GAM (Beck et al., 2018b); e) LV percent rainforest pollen with fitted GAM; f) Dove Lake rainforest:sclerophyll ratio with fitted GAM (Mariani et al., 2018); and g) Paddy's Lake percent rainforest pollen with fitted GAM (Beck et al., 2017). (For interpretation of the references to colour in this figure legend, the reader is referred to the Web version of this article.)

deposition of organic and inorganic terrestrial material into Lake Vera (Fig. 8b and d). Fire mobilises sediments and rainfall following fire, and erodes terrigenous materials (organic and inorganic) into nearby waterways (di Folco and Kirkpatrick, 2011; Morris et al., 2015). These fire-driven erosion events are consistent with increased abundance of *D. stelligera* (Fig. 8c). *D. stelligera* is a complex species with affinities to nutrient, conductivity and mixing depth (Fritz et al., 2019; Malik and Saros, 2016; Saros and Anderson, 2015; Saros et al., 2016). Our results show *D. stelligera* is favoured by lower lake levels and could indicate decreased mixing depth with increased deposition of organic and inorganic terrestrial material (Fig. 8b and d). *D. stelligera* prefers shallower mixing depths compared to heavier siliceous diatoms that require more light penetration and strong mixing (*Aulacoseira* spp.) (Fig. 4f) (Saros and Anderson, 2015; Saros et al., 2012, 2014, 2016). Potential lower mixing depth, via less light penetration, of the lake could be caused

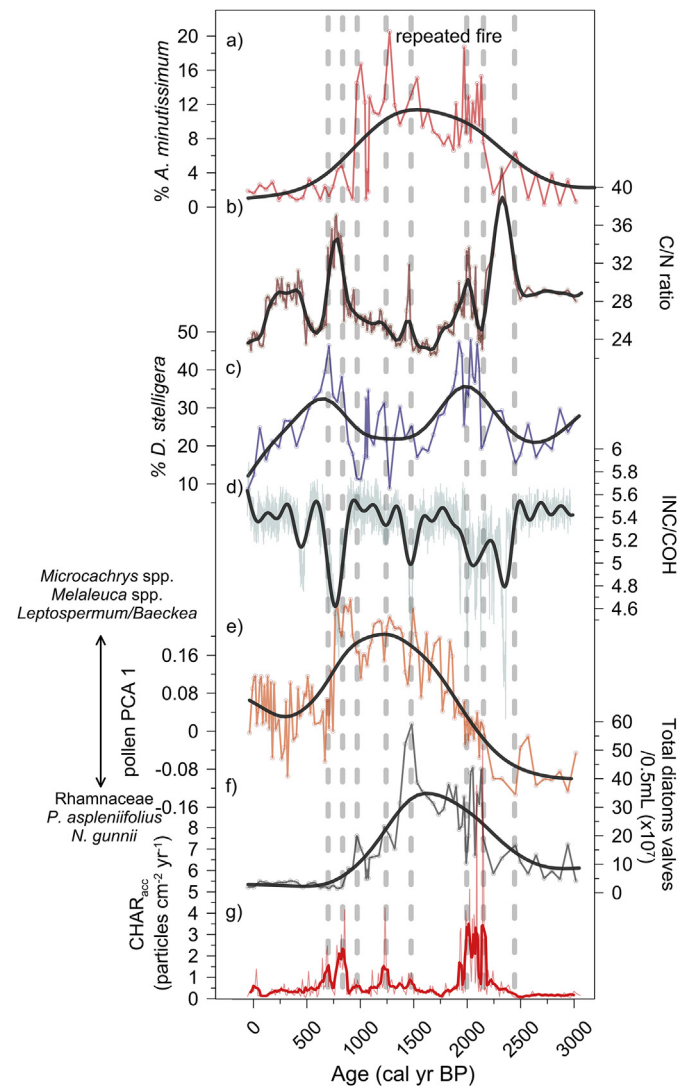


Fig. 8. Summary figure of Lake Vera a) % *Achnanthidium minutissimum* (red) with fitted GAM; b) Carbon/Nitrogen ratio (brown) with fitted GAM; c) percent abundance of *Discostella stelligera* (blue) with fitted GAM; d) XRF INC/COH ratio (green) with fitted GAM; e) pollen PCA axis 1 (orange) with fitted GAM; f) total diatom valve concentration (/0.5 mL $\times 10^7$) (dark grey) with fitted GAM; and g) macroscopic charcoal accumulation (particles $\text{cm}^{-2} \text{yr}^{-1}$) (light red) with fitted weighted average (window width = 5) (red). Grey dashed lines indicate peaks in CHAR_{acc} . (For interpretation of the references to colour in this figure legend, the reader is referred to the Web version of this article.)

by (1) elevated concentrations of dissolved solids or humic content during periods of low lake levels or (2) increased deposition of inorganics (low INC/COH; Fig. 4a) and detrital elements (high XRF PCA 1; Fig. 4c and Supplementary Data) caused by increased erosion via burning (Gell and Reid, 2014; Reid et al., 2007; Steane and Tyler, 1982; Wetzel, 1992).

Initially, the onset of fire (ca. 2.6 ka) causes an increase in terrestrial inputs (C/N at ca. 2.6 ka) and diatom productivity (ca. 2.6 ka), followed by peaks in charcoal and diatom concentration at ca. 2.3 ka (Fig. 8). However, continued fire disturbance (peaks between ca. 2.3 to 0.7 ka; Fig. 8) results in a decline in productivity (at ca. 1.4 ka) plummeting before the final peak in fire at ca. 0.7 ka (Fig. 8). Diatom productivity is driven by multiple factors such as nutrient and sediment inputs, available Si, light and temperature (Battarbee et al., 2001; Bradbury et al., 2002). Our results suggest fire mobilises sediments eroding organic and nutrient rich terrigenous material

into Lake Vera (C/N and INC/COH; Fig. 8b and d) causing an increase in diatom concentration (Fig. 8f). *A. minutissimum*, *A. subexigua*, *Psammothidium didymum*, *Brachysira styriaca*, and *Fragilaria capucina* are taxa with increasing abundance during this productive phase. These benthic species are tolerant of alkaline and turbulent waters (Figs. 4 and 6) (Korholka et al., 1996; Law et al., 2015; Peterson and Stevenson, 1992; Robinson and Rushforth, 1987). *A. minutissimum*, a cosmopolitan species, is the most abundant diatom taxa of this assemblage and is characteristic of oligotrophic waters with a tolerance for hydrological disturbance and metal deposition (Cantonati et al., 2014; Giles et al., 2018; Passy, 2007; Peterson and Stevenson, 1992; Ponader and Potapova, 2007; Vacht et al., 2014). *D. stelligera* also increases in abundance at ca. 2.3 ka suggesting light limitation from increased terrigenous material. This anomalous assemblage and high diatom concentration indicates an increase in diatom productivity and a disturbed (low-light and turbid) alkaline environment.

Diatom concentration falls before the last charcoal peak in the Lake Vera record (ca. 0.7 ka) (Fig. 8) and alkaline disturbance diatoms are replaced by acidic, oligotrophic, dystrophic benthic diatoms (*Eunotia* spp. and *F. elongatissima*). Slight pulses in productivity occur with burning following the decline in diatom concentration (ca. 1.2 and 0.9 ka) but the final fire events do not influence diatom productivity (Fig. 8). Repeated fire disturbance removes terrestrial biomass (Bixby et al., 2015), promotes sclerophyllous vegetation and kills pyrophobic vegetation (rainforest vegetation; Figs. 4 and 8e) creating gaps in the canopy for sunlight to reach the forest floor where ferns and pioneer rainforest, *P. asplenijfolius* (Fig. 4e and j), can proliferate (Barker and Kirkpatrick, 1994; Barlow et al., 2003; Cochrane et al., 1999; Cohen, 2003; Nakagawa et al., 2000). These most recent changes (ca. 0.9 ka to present) suggest a more open canopy at Lake Vera with a low productive oligotrophic acidic aquatic environment, the result of repeated fire disturbance (Beck et al., 2018a).

5.2. Regional climate impacts on aquatic environments

Our analysis from Lake Vera is the third coupled terrestrial-aquatic reconstruction spanning the Holocene epoch from the cool temperate environment of western Tasmania, the other two being from Paddy's Lake (Beck et al., 2018b) and Dove Lake (Mariani et al., 2018). A comparison of these three coupled studies reveals three key insights into the nature of long-term (multi-millennial scale) terrestrial-aquatic ecosystem dynamics in this region: (1) terrestrial and aquatic ecosystem change was tightly coupled at each site through the Holocene; (2) a remarkably coherent trend across sites in this region reveals long-term climatic change as the key driver of multi-millennial scale terrestrial and aquatic ecosystem dynamics through the Holocene in this region; and (3) a primarily indirect influence of climate over aquatic ecosystem dynamics that is mediated via tightly coupled climate-driven vegetation-soil dynamics.

In the terrestrial environments at each of these sites, the aquatic ecosystem responds to changes in rainforest associated with changes in hemispheric-scale hydroclimate (Fig. 7a) (Mariani and Fletcher, 2017). The principal mechanism of terrestrial-aquatic links at each site is via changes in the accumulation of peat under rainforest vegetation. The development of deep peat profiles under undisturbed rainforest are fostered by increasing moisture under enhanced SWW circulation over the region. The accumulation of catchment peat content under a wetter climate (enhanced SWW circulation) results in lake ontogenetic processes (increased acidity, dystrophy and/or nutrient availability) (Beck et al., 2018b; Mariani et al., 2018). Interestingly the apparent primary driver of aquatic ecosystem change (pH, dystrophy or nutrient availability), varies

across sites and aquatic proxies. At Dove Lake and Lake Vera, diatoms were employed and reveal changes in pH and dystrophy, whereas nutrient availability is the driver of change within Paddy's Lake where cladocerans were analysed (Fig. 7). While further analysis of various coupled terrestrial-aquatic proxies from the same site is required to disentangle the influence of proxy selection, long-term aquatic ecosystem change at all sites was driven by climate-mediated changes in the terrestrial vegetation-soil system.

The region-wide pattern of climate-driven terrestrial-aquatic ecosystem change persisted through the mid-to late-Holocene and shifts to a more variable and drier hydroclimate. Increased regional charcoal, indicative of drying, is coeval with declines in rainforest at all sites (Fig. 7). Differing biogeography of these lakes caused some variation in aquatic response. For instance, Lake Vera is rainforested, while Dove Lake has a wet sclerophyll forest and Paddy's Lake is characterised by subalpine heath. Paddy's Lake is the highest elevation in a northern locality with an isolated catchment compared to Lake Vera and Dove Lake that have highly connected catchments. Interestingly, the regional pattern is consistent (aquatic ecosystems are indirectly driven by climate), yet each site displays an idiosyncratic terrestrially mediated response to climate change through this phase. Dominance of diatom *D. stelligera* at Lake Vera indicates a drop in lake level (Fig. 7b), while Dove Lake shows increases in *Aulacoseira* spp. associated with more light penetration from reduced humic acid input and lower dystrophy (Fig. 7c) (Mariani et al., 2018). Paddy's Lake is dominated by pelagic cladoceran, *Bosmina meridionalis*, indicating a reduction in available nutrients within the lake (Fig. 7d) (Beck et al., 2018b) as a fire-driven increase in sclerophyllous vegetation resulted in the development of nutrient deficient organosols (Bowman and Jackson, 1981; Bridle et al., 2003). The earlier response at Paddy's Lake reflects the high sensitivity of this site to the initial changes in the ENSO system between ca. 7 to 6 ka (Paddy's Lake lies in a zone of strong correlation between rainfall and ENSO in the modern climate unlike the other sites; Fig. 1) (Beck et al., 2018b). While the terrestrial-aquatic interactions between sites differ, each site shows a lagged aquatic response to the corresponding terrestrial environment, suggesting indirect climate influences (Beck et al., 2018b), regardless of proxy type or catchment biogeography.

5.3. Impacts of fire on aquatic ecosystems

The influence of fire over aquatic ecosystems is complex. In western Tasmania, fire activity is modulated by people and driven by changes in hydroclimate (Fletcher et al., 2015; Fletcher and Thomas, 2010; Mariani and Fletcher, 2017). Fires can destroy vegetation and associated peat layers, resulting in increased erosion (Fletcher et al., 2014) and lake alkalinity (Beck et al., 2018a; Haberle et al., 2006; Korholka et al., 1996; Renberg et al., 1993b). While fire can initially mobilise nutrients (N and P) from soils (Kirkpatrick and Dickinson, 1984; Leys et al., 2016), the removal of organic soils and biomass caused by fire can result in a long-term loss of available nutrients from a catchment system (Bixby et al., 2015; Dunnette et al., 2014; Morris et al., 2015). Importantly, there is evidence that nutrient pulses associated with fire cannot be fully exploited by aquatic organisms due to corresponding inputs of inorganic material affecting light availability (Brown, 2016; Klose et al., 2015).

At Lake Vera it appears fire initially stimulates algal production, but over time continued fire disturbance in the catchment causes the aquatic ecosystem to shift into an oligotrophic unproductive state. Initial burning at ca. 2.6 ka (Fig. 8g) releases nutrients and organic material into the lake, i.e. C/N ca. 2.6 ka (Fig. 8b), stimulating diatom production (ca. 2.6 ka; Fig. 8f). However, after repeated burning (ca. 2.3 to 0.7 ka) diatom production decreases

before burning declines (following ca. 1.4 ka) (Fig. 7f). Heavy rain following fire is known to strip important soil layers (Bowman and Jackson, 1981; di Folco and Kirkpatrick, 2011) and repeated burning may not allow enough time for peat soils to recover; thus, permanently reducing the long-term available nutrient pool for aquatic systems. Further, in Tasmania, the role of fire over vegetation structure has altered available nutrients on the landscape. Increases in sclerophyll vegetation from fire produce thinner organic soil profiles with a lower nutrient status than rainforest vegetation (Bowman et al., 1986; Bradstock, 2010; Murphy et al., 2010). Thus, a shift from rainforest to sclerophyll vegetation can drive a reduction in nutrient input to lakes that impact the aquatic ecosystem trophic status (Beck et al., 2018b).

Fire activity also alters lake water alkalinity and our findings from Lake Vera suggest it may also potentially lower mixing depth. Ash deposition increases the base cation content of a lake (Korhola et al., 1996; Korsman and Segerstrom, 1998), buffering acidity and increasing the abundance of alkaline diatom taxa (i.e. *Achnanthes* type species; Figs. 4 and 6). Fire also releases terrestrial organic and inorganic material from the catchment (di Folco and Kirkpatrick, 2011; González-Pérez et al., 2004; Ketterings et al., 2000; Korhola et al., 1996; Kutiel and Inbar, 1993) that can decrease light penetration into a lake. Our results suggest that the deposition of terrestrial material may restrict light availability and favour taxa with lower mixing depth preferences, i.e. *Discostella stelligera* (Fig. 8c) (Saros and Anderson, 2015; Saros et al., 2012). Over time repeated fire disturbance and erosion may decrease light penetration and prevent the uptake of available nutrients, and thus, productivity of aquatic organisms (Brown, 2016; Klose et al., 2015). Therefore our findings suggest the impacts of fire on aquatic ecosystems are complex, altering algal production, pH, nutrients and lake mixing, and these factors are, in turn, determined by catchment characteristics such as soil and vegetation type (Fig. 8).

6. Conclusions

The multi-proxy Lake Vera record shows a complex history of ontogenetic processes driven by hemispheric-scale hydroclimate trends during the early to mid-Holocene. With the onset of fire, the aquatic ecosystem response to catchment processes is altered and fire becomes the primary driver of aquatic ecosystem response via its influence on terrestrial inputs into water bodies. Enhanced precipitation from a hemisphere-wide increase in SWW flow over the mid-latitudes (from ca. 9 to 6.5 ka) resulted in high lake levels at our study site, with the lake environment characterised by turbulent and oligotrophic water. Increased rainforest development under high rainfall resulted in the development of deep catchment peat profiles and an increase in humic acid input into the lake, producing a dystrophic and acidic lake environment. These lake ontogenetic processes appear to be occurring across multiple sites in western Tasmania during the Holocene indicating a tight regional coupling between climate and terrestrially mediated aquatic ecosystem change. Regional drying (from ca. 4.0 ka) results in a drop in lake level and change in mixing depth at our site that favours *D. stelligera*. These climate related responses in the aquatic environment are consistent with the regional palaeolimnology. Though the three sites examined have different biogeography, they show consistent trends in terrestrial mediated aquatic ecosystem responses to climate.

Fire disturbance in the Lake Vera catchment (ca. 2.3 ka) resulted in increased input of organic and inorganic terrestrial material and a more productive disturbed alkaline aquatic environment. The onset of burning is likely the result of continued drying permitting the influence of anthropogenic fires into this rainforest environment. Repeated fire disturbance eventually resulted in a diatom

shift to an acidic oligotrophic lake environment with low productivity (at ca. 0.9 ka). Our data indicate the key role of climate and fire in aquatic ecosystem dynamics that must be considered when assessing the potential impact of future climate and fire changes under anthropogenic climate and land use change.

Acknowledgements

The financial support for this project comes from the Australian Research Council (award: #DI110100019 and IN140100050) and Australian Institute of Nuclear Science and Engineering (award: ALNGRA12003P). Kristen K. Beck would like to thank the Albert Shimmens Fund for financial assistance. We thank the Tasmania National Parks and Wildlife Service and the Tasmanian Aboriginal Community for their support and allowing us to work on their lands. As well, thank you to Michela Mariani, Anthony Romano, Coralie Tate, and Valentina Vanghi for their assistance in the field. We would like to acknowledge Gavin L. Simpson for his assistance and support with the statistical analyses, Brent Wolfe and his laboratory at University of Waterloo, Canada (adjunct with Wilfrid Laurier University, Waterloo, Canada), and Mark Rollog from the University of Adelaide, Australia for their assistance with isotopic analysis and interpretation. We would like to thank the two reviewers for their feedback and support on this manuscript. All data presented in the tables, figures and Supplementary data will be made publicly available on Neotoma (<https://www.neotomadb.org/>) upon publication.

Appendix A. Supplementary data

Supplementary data to this article can be found online at <https://doi.org/10.1016/j.quascirev.2019.105892>.

References

- Appleby, P., 2001. Chronostratigraphic Techniques in Recent Sediments, Tracking Environmental Change Using Lake Sediments. Kluwer Academic Publishers, Dordrecht, The Netherlands, pp. 171–203.
- Aquatic Research Instruments, 2018. Universal Percussion Corer. Aquatic Research Instruments, Indiana, USA.
- Augustinus, P., Cochran, U., Kattel, G., D'Costa, D., 2012. Late Quaternary paleolimnology of Onepoto maar, Auckland, New Zealand: implications for the drivers of regional paleoclimate. *Quat. Int.* 253, 18–31.
- Ball, B.A., Kominoski, J.S., Adams, H.E., Jones, S.E., Kane, E.S., Loecke, T.D., Mahaney, W.M., Martina, J.P., Prather, C.M., Robinson, T.M.P., 2010. Direct and terrestrial vegetation-mediated effects of environmental change on aquatic ecosystem processes. *Bioscience* 60, 590–601.
- Barker, P.C.J., Kirkpatrick, J.B., 1994. *Phyllocladus aspleniifolius*: variability in the population structure, the regeneration niche and dispersion patterns in Tasmanian forests. *Aust. J. Bot.* 42, 163–190.
- Barlow, J., Peres, C.A., Lagan, B.O., Haugaaen, T., 2003. Large tree mortality and the decline of forest biomass following Amazonian wildfires. *Ecol. Lett.* 6, 6–8.
- Barr, C., Tibby, J., Leng, M.J., Tyler, J.J., Henderson, A.C.G., Overpeck, J.T., Simpson, G.L., Cole, J.E., Phipps, S.J., Marshall, J.C., McGregor, G.B., Q. Hua, Q., McRobie, F.H., 2019. Holocene El Niño—southern oscillation variability reflected in subtropical Australian precipitation. *Sci. Rep.* 9, 1627.
- Battarbee, R.W., 1986. Diatom analysis. In: Berglund, B.E. (Ed.), *Handbook Palaeoecology and Palaeohydrology*. John Wiley & Sons, Chichester, pp. 527–570.
- Battarbee, R.W., 2000. Palaeolimnological approaches to climate change, with special regard to the biological record. *Quat. Sci. Rev.* 19, 107–124.
- Battarbee, R.W., Jones, V.J., Cameron, N.G., Bennion, H., Carvalho, L., Juggins, S., 2001. Diatoms. In: Smol, J.P., Birks, H.J.B., Last, W.M. (Eds.), *Tracking Environmental Change Using Lake Sediments: Terrestrial, Algal and Siliceous Indicators*. Kluwer, Dordrecht, pp. 155–202.
- Beck, K.K., Fletcher, M.-S., Gadd, P.S., Heijnis, H., Jacobsen, G.E., 2017. An early onset of ENSO influence in the extra-tropics of the southwest Pacific inferred from a 14,600 year high resolution multi-proxy record from Paddy's Lake, northwest Tasmania. *Quat. Sci. Rev.* 157, 164–175.
- Beck, K.K., Fletcher, M.S., Gadd, P.S., Heijnis, H., Saunders, K.M., Simpson, G.L., Zawadzki, A., 2018a. Variance and rate-of-change as early warning signals for a critical transition in an aquatic ecosystem state: a test case from Tasmania, Australia. *J. Geophys. Res. Biogeosci.* 123, 495–508.
- Beck, K.K., Fletcher, M.S., Kattel, G., Barry, L.A., Gadd, P.S., Heijnis, H., Jacobsen, G., Saunders, K.M., 2018b. The indirect response of an aquatic ecosystem to long

- term climate-driven terrestrial vegetation in subalpine temperate Tasmania. *J. Biogeogr.* 45, 713–725.
- Bennion, H., Simpson, G.L., Goldsmith, B.J., 2015. Assessing degradation and recovery pathways in lakes impacted by eutrophication using the sediment record. *Front. Ecol. Evolut.* 3, 94.
- Birks, H., 1997. Reconstructing Environmental Impacts of Fire from the Holocene Sediment Record, *Sediment Records of Biomass Burning and Global Change*. Springer, pp. 295–311.
- Birks, H.H., Birks, J.H.B., 2006. Multi-proxy studies in palaeolimnology. *Veg. Hist. Archaeobotany* 15, 235–251.
- Bixby, R.J., Cooper, S.D., Gresswell, R.E., Brown, L.E., Dahm, C.N., Dwire, K.A., 2015. Fire effects on aquatic ecosystems: an assessment of the current state of the science. *Freshw. Sci.* 34, 1340–1350.
- Blaauw, M., Christen, J.A., 2013. Bacon Manual- v2.2, pp. 1–11.
- Bowman, D., 1998. The impact of Aboriginal landscape burning on the Australian biota. *New Phytol.* 140, 385–410.
- Bowman, D., Brown, M.J., 1986. Bushfires in Tasmania: a botanical approach to anthropological questions. *Archaeol. Ocean.* 21, 166–171.
- Bowman, D., Jackson, W., 1981. Vegetation succession in southwest Tasmania. *Search* 12, 358–362.
- Bowman, D., Maclean, A.R., Crowden, R.K., 1986. Vegetation-soil relations in the lowlands of south-west Tasmania. *Aust. J. Ecol.* 11, 141–153.
- Bowman, D., Wood, S.W., 2009. Fire-driven Land Cover Change in Australia and WD Jackson's Theory of the Fire Ecology of Southwest Tasmania, *Tropical Fire Ecology*. Springer, Berlin Heidelberg, pp. 87–111.
- Bowman, D.M.J.S., Balch, J., Artaxo, P., Bond, W.J., Cochrane, M.A., D'Antonio, C.M., DeFries, R., Johnston, F.H., Keeley, J.E., Krawchuk, M.A., Kull, C.A., Mack, M., Moritz, M.A., Pyne, S., Roos, C.I., Scott, A.C., Sodhi, N.S., Swetnam, T.W., 2011. The human dimension of fire regimes on Earth. *J. Biogeogr.* 38, 2223–2236.
- Bradbury, P., Cumming, B., Laird, K., 2002. A 1500-year record of climatic and environmental change in ElkLake, Minnesota III: measures of past primary productivity. *J. Paleolimnol.* 27, 321–340.
- Bradbury, P.J., 1986. Late Pleistocene and Holocene paleolimnology of two mountain lakes in western Tasmania. *Palaio* 1, 381–388.
- Bradstock, R.A., 2010. A biogeographic model of fire regimes in Australia: current and future implications. *Glob. Ecol. Biogeogr.* 19, 145–158.
- Bridle, K.L., Cullen, P.J., Russell, M., 2003. Peatland Hydrology, Fire Management and Holocene Fire Regimes in Southwest Tasmanian Blanket Bogs, Earth Science Section, Nature Conservation Report No. 03/07. Nature Conservation Branch of the Department of Primary Industries, Water and Environment, Hobart, Tasmania, Australia, p. 97.
- Brown, M.J., Crowden, R.K., Jarman, S.J., 1982. Vegetation of an alkaline pan — acidic peat mosaic in the hardwood river valley, Tasmania. *Aust. J. Ecol.* 7, 3–12.
- Brown, S., 2016. Multi-proxy Holocene Fire History Reconstruction in Beartooth Mountains, Wyoming. Department of Earth and Environmental Systems. Indiana State University, Indiana, USA.
- Buckney, R., Tyler, P., 1973. Chemistry of some sedgeland waters: lake Pedder, south-west Tasmania. *Aust. J. Mar. Freshw. Res.* 24, 267–273.
- Cantonati, M., Angeli, N., Virtanen, L., Wojtal, A.Z., Gabrielli, J., Falasco, E., Lavoie, I., Morin, S., Marchetto, A., Fortin, C., Smirnova, S., 2014. Achnanthidium minutissimum (Bacillariophyta) valve deformities as indicators of metal enrichment in diverse widely-distributed freshwater habitats. *Sci. Total Environ.* 475, 201–215.
- Cochrane, M.A., Alencar, A., Schulze, M.D., Souza Jr, C.M., Nepstad, D.C., Lefebvre, P., Davidson, E.A., 1999. Positive feedbacks in the fire dynamic of closed canopy tropical forests. *Science* 284, 1832–1835.
- Cohen, A.S., 2003. *Paleolimnology: the History and Evolution of Lake Systems*. Oxford University Press, USA.
- Croudace, I.W., Rothwell, R.G., 2015. *Micro-Xrf Studies of Sediment Cores: Applications of a Non-destructive Tool for the Environmental Sciences*. Springer Science + Business Media Dordrecht, Dordrecht Heidelberg New York London.
- di Folco, M.-B., Kirkpatrick, J.B., 2011. Topographic variation in burning-induced loss of carbon from organic soils in Tasmanian moorlands. *Catena* 87, 216–225.
- DPIPWE, 2016. Tasmanian wilderness world heritage area management plan. In: Water and Environment. Department of Primary Industries, Parks, Water and Environment, Hobart, Tasmania.
- Dunnette, P.V., Higuera, P.E., McLauchlan, K.K., Derr, K.M., Briles, C.E., Keefe, M.H., 2014. Biogeochemical impacts of wildfires over four millennia in a Rocky Mountain subalpine watershed. *New Phytol.* 203, 900–912.
- Faegri, K., Iversen, J., 1989. *Textbook of Pollen Analysis*, 4 ed. John Wiley & Sons Ltd, London, Great Britain.
- Flannigan, M.D., Krawchuk, M.A., de Groot, W.J., Wotton, M.B., Gowman, L.M., 2009. Implications of changing climate for global wildland fire. *Int. J. Wildland Fire* 18, 483–507.
- Fletcher, M.-S., 2015. Mast seeding and the El Niño-southern oscillation: a long-term relationship? *Plant Ecol.* 216, 527–533.
- Fletcher, M.-S., Benson, A., Bowman, D.M.J.S., Gadd, P.S., Heijnis, H., Mariani, M., Saunders, K.M., Wolfe, B.B., Zawadzki, A., 2018a. Centennial-scale trends in the Southern Annular Mode revealed by hemisphere-wide fire and hydroclimatic trends over the last 2400 years. *Geology* 46, 363–366.
- Fletcher, M.-S., Benson, A., Heijnis, H., Gadd, P.S., 2015. Changes in biomass burning mark the onset an ENSO-influenced climate regime at 42° S in southwest Tasmania, Australia. *Quat. Sci. Rev.* 122, 222–232.
- Fletcher, M.-S., Bowman, D., Whitlock, C., Mariani, M., Stahle, L.N., 2018b. The changing role of fire in conifer-dominated temperate rainforest through the last 14,000 years. *Quat. Sci. Rev.* 182, 37–47.
- Fletcher, M.-S., Wolfe, B.B., Whitlock, C., Pompeani, D.P., Heijnis, H., Haberle, S.G., Gadd, P.S., Bowman, D., 2014. The legacy of mid-Holocene fire on a Tasmanian montane landscape. *J. Biogeogr.* 41, 476–488.
- Fletcher, M.S., Moreno, P., 2012. Have the Southern Westerlies changed in a zonally symmetric manner over the last 14,000 years? A hemisphere-wide take on a controversial problem. *Quat. Int.* 253, 32–46.
- Fletcher, M.S., Moreno, P.I., 2011. Zonally symmetric changes in the strength and position of the Southern Westerlies drove atmospheric CO₂ variations over the past 14 ky. *Geology* 39, 419–422.
- Fletcher, M.S., Thomas, I., 2010. The origin and temporal development of an ancient cultural landscape. *J. Biogeogr.* 37, 2183–2196.
- Foged, N., 1978. Diatoms in Eastern Australia. *J. Cramer, Vaduz*.
- Fox-Hughes, P., Harris, R., Lee, G., Grose, M., Bindoff, N., 2014. Future fire danger climatology for Tasmania, Australia, using a dynamically downscaled regional climate model. *Int. J. Wildland Fire* 23, 309–321.
- Fritz, S.C., Anderson, N.J., 2013. The relative influences of climate and catchment processes on Holocene lake development in glaciated regions. *J. Paleolimnol.* 49, 349–362.
- Fritz, S.C., Benito, X., Steinitz-Kannan, M., 2019. Long-term and regional perspectives on recent change in lacustrine diatom communities in the tropical Andes. *J. Paleolimnol.* 61, 251–262.
- Garreaud, R.D., 2007. Precipitation and circulation covariability in the extratropics. *J. Clim.* 20, 4789–4797.
- Gell, P., Reid, M., 2014. Assessing change in floodplain wetland condition in the Murray Darling Basin, Australia. *Anthropocene* 8, 39–45.
- Gell, P.A., 1999. An Illustrated Key to Common Diatom Genera from Southern Australia. Cooperative Research Centre for Freshwater Ecology, Thuringowa, NSW.
- Giles, M.P., Michelutti, N., Grooms, C., Smol, J.P., 2018. Long-term limnological changes in the Ecuadorian páramo: comparing the ecological responses to climate warming of shallow waterbodies versus deep lakes. *Freshw. Biol.* 63, 1316–1325.
- González-Pérez, J.A., González-Vila, F.J., Almendros, G., Knicker, H., 2004. The effect of fire on soil organic matter—a review. *Environ. Int.* 30, 855–870.
- Haberle, S.G., Tibby, J., Dimitriadis, S., Heijnis, H., 2006. The impact of European occupation on terrestrial and aquatic ecosystem dynamics in an Australian tropical rain forest. *J. Ecol.* 94, 987–1002.
- Harris, R.M.B., Beaumont, L.J., Vance, T.R., Tozer, C.R., Remenyi, T.A., Perkins-Kirkpatrick, S.E., Mitchell, P.J., Nicotra, A.B., McGregor, S., Andrew, N.R., Letnic, M., Kearney, M.R., Wernberg, T., Hustley, L.B., E.C.L., Fletcher, M.-S., R.K.M., Woodward, C.A., Williamson, G., Duke, N.C., Bowman, D.M.J.S., 2018. Biological responses to the press and pulse of climate trends and extreme events. *Nat. Clim. Chang.* 8, 579–587.
- Hastie, T., Tibshirani, R., 1990. *Generalized Additive Models*. Chapman and Hall/CRC United States.
- Hogg, A., Hua, Q., Blackwell, P., Niu, M., Buck, C., Guilderson, T., Zimmerman, S., 2013. SHCal13 southern hemisphere calibration, 0–50,000 years cal BP. *Radiocarbon* 55, 1889–1903.
- Holz, A., Wood, S.W., Veblen, T.T., Bowman, D., 2015. Effects of high severity fire drove the population collapse of the subalpine Tasmanian endemic conifer Athrotaxis cupressoides. *Glob. Chang. Biol.* 21, 445–458.
- Hopf, F.V.L., Colhoun, E.A., Barton, C.E., 2000. Late-glacial and Holocene record of vegetation and climate from cynthia Bay, lake St clair, Tasmania. *J. Quat. Sci.* 15, 725–732.
- Huvane, J.K., Whitehead, D.R., 1996. The paleolimnology of North Pond: watershed-lake interactions. *J. Paleolimnol.* 16, 323–354.
- Jackson, W., 1968. Fire, air, water and earth—an elemental ecology of Tasmania. In: Proceedings of the Ecological Society of Australia, Canberra, Australia, pp. 9–16.
- John, J., 1983. The diatom flora of the Swan River estuary, Western Australia. *Bibl. Phycol.* 1–358. ISBN: 3768213609.
- John, J., 2016. *Diatoms from Stradbroke and Fraser Islands, Australia: Taxonomy and Biogeography*. Koeltz Botanical Books, Germany.
- John, J., 2018. *Diatoms of Tasmania: Taxonomy and Biogeography*. Koeltz Botanical Books, Kapellenbergstr.
- Ketterings, Q.M., Bigham, J.M., Laperche, V., 2000. Changes in soil mineralogy and texture caused by slash-and-burn fires in Sumatra, Indonesia. *Soil Sci. Soc. Am. J.* 64, 1108–1117.
- Kilroy, C., Sabbe, K., Bergey, E.A., Vyverman, W., Lowe, R., 2003. New species of Frigilariforma (Bacillariophyceae) from New Zealand and Australia. *N. Z. J. Bot.* 41, 535–554.
- Kirkpatrick, J.B., Dickinson, K.J.M., 1984. The impact of fire on Tasmanian alpine vegetation and soils. *Aust. J. Bot.* 32, 613–629.
- Kitchener, A., Harris, S., 2013. From Forest to Fjeldmark: Description of Tasmania's Vegetation, 2 ed. Department of Primary Industries, Parks, Water and Environment, Tasmania.
- Klose, K., Cooper, S.D., Bennett, D.M., 2015. Effects of wildfire on stream algal abundance, community structure, and nutrient limitation. *Freshw. Sci.* 34, 1494–1509.
- Kociolek, J.P.S., Sarah, A., Sabbe, K., Vyverman, W., 2004. New *Comphonema* (Bacillariophyta) species from Tasmania. *Phycologia* 43, 427–444.
- Korhola, A., Virkanen, J., Tikkainen, M., Blom, T., 1996. Fire-induced pH rise in a naturally acid hill-top lake, southern Finland: a palaeoecological survey. *J. Ecol.* 84, 257–265.
- Korsman, T., Segerstrom, U., 1998. Forest fire and lake-water acidity in a northern

- Swedish boreal area: Holocene changes in lake-water quality at Makkasson. *J. Ecol.* 86, 113–124.
- Krawchuk, M.A., Moritz, M.A., Parisien, M.-A., Van Dorn, J., Hayhoe, K., 2009. Global pyrogeography: the current and future distribution of wildfire. *PLoS One* 4, e5102.
- Kutiel, P., Inbar, M., 1993. Fire impacts on soil nutrients and soil erosion in a Mediterranean pine forest plantation. *Catena* 20, 129–139.
- Law, A.C., Anderson, N.J., McGowan, S., 2015. Spatial and temporal variability of lake ontogeny in south-western Greenland. *Quat. Sci. Rev.* 126, 1–16.
- Leys, B., Higuera, P.E., McLauchlan, K.K., Dunnette, P.V., 2016. Wildfires and geochemical change in a subalpine forest over the past six millennia. *Environ. Res. Lett.* 11, 125003.
- Macphail, M.K., 1979. Vegetation and climates in southern Tasmania since the last glaciation. *Quat. Res.* 11, 306–341.
- Malik, H.I., Saros, J.E., 2016. Effects of temperature, light and nutrients on five *Cyclotella* sensu lato taxa assessed with in situ experiments in arctic lakes. *J. Plankton Res.* 38, 431–442.
- Mariani, M., Beck, K.K., Fletcher, M.S., Gell, P., Saunders, K.M., Gadd, P., Chisari, R., 2018. Biogeochemical responses to Holocene hydroclimate fluctuations in the Tasmanian world heritage area, Australia. *J. Geophys. Res. Biogeosci.* 123, 1610–1624.
- Mariani, M., Connor, S.E., Fletcher, M.S., Theuerkauf, M., Kuneš, P., Jacobsen, G., Saunders, K.M., Zawadzki, A., 2017. How old is the Tasmanian cultural landscape? A test of landscape openness using quantitative land-cover reconstructions. *J. Biogeogr.* 44, 2410–2420.
- Mariani, M., Fletcher, M.S., 2016. The Southern Annular Mode determines interannual and centennial-scale fire activity in temperate southwest Tasmania, Australia. *Geophys. Res. Lett.* 43, 1702–1709.
- Mariani, M., Fletcher, M.S., 2017. Long-term climate dynamics in the southern extratropics revealed from sedimentary charcoal analysis. *Quat. Sci. Rev.* 173, 187–192.
- Mariani, M., Fletcher, M.S., Holz, A., Nyman, P., 2016. ENSO controls interannual fire activity in southeast Australia. *Geophys. Res. Lett.* 43, 10891–10900.
- Mills, K., Schillereff, D., Talbot, É., Gell, P., Anderson, J.N., Arnaud, F., Dong, X., Jones, M., McGowan, S., Massafarro, J., Moorhouse, H., Perez, L., Ryves, D.B., 2017. Deciphering long term records of natural variability and human impact as recorded in lake sediments: a palaeolimnological puzzle. *Wiley Interdiscip. Rev.: Water* 4, 1195.
- Moritz, M.A., Parisien, M.-A., Batllori, E., Krawchuk, M.A., Dorn, J., Ganz, D.J., Hayhoe, K., 2012. Climate change and disruptions to global fire activity. *Ecosphere* 3, 1–22.
- Morris, J.L., McLauchlan, K.K., Higuera, P.E., 2015. Sensitivity and complacency of sedimentary biogeochemical records to climate-mediated forest disturbances. *Earth Sci. Rev.* 148, 121–133.
- Murphy, B.P., Bradstock, R.A., Boer, M.M., Carter, J., Cary, G.J., Cochrane, M.A., Fensham, R.J., Russell-Smith, J., Williamson, G.J., Bowman, D., 2013. Fire regimes of Australia: a pyrogeographic model system. *J. Biogeogr.* 40, 1048–1058.
- Murphy, B.P., Paron, P., Prior, L.D., Boggs, G.S., Franklin, D.C., Bowman, D., 2010. Using generalized autoregressive error models to understand fire–vegetation–soil feedbacks in a mulga–spinifex landscape mosaic. *J. Biogeogr.* 37, 2169–2182.
- Nakagawa, M., Tanaka, K., Nakashizuka, T., Ohkubo, T., Kato, T., Maeda, T., Sato, K., Miguchi, H., Nagamasu, H., Ogino, K., Teo, S., Hamid, A.A., Seng, L.H., 2000. Impact of severe drought associated with the 1997–1998 El Niño in a tropical forest in Sarawak. *J. Trop. Ecol.* 16, 355–367.
- Neil, K., Gajewski, K., 2018. An 11,000-yr record of diatom assemblage responses to climate and terrestrial vegetation changes, southwestern Québec. *Ecosphere* 9, e02505.
- Nesje, A., 1992. A piston corer for lacustrine and marine sediments. *Arct. Alp. Res.* 257–259.
- Oksanen, J., Blanchet, F.G., Kindt, R., Legendre, P., Minchin, P.R., O'Hara, R.B., Simpson, G.L., Solymos, P., Stevens, M.H.H., Wagner, H., 2019. Package: vegan, community ecology package, 2.5–4. In: *Ordination Methods, Diversity Analysis and Other Functions for Community and Vegetation Ecologists*.
- Passy, S.I., 2007. Diatom ecological guilds display distinct and predictable behavior along nutrient and disturbance gradients in running waters. *Aquat. Bot.* 86, 171–178.
- Perren, B.B., Axford, Y., Kaufman, D.S., 2017. Alder, nitrogen, and lake ecology: terrestrial-aquatic linkages in the postglacial history of Lone Spruce pond, southwestern Alaska. *PLoS One* 12, e0169106.
- Peterson, C.G., Stevenson, R.J., 1992. Resistance and resilience of lotic algal communities: importance of disturbance timing and current. *Ecology* 73, 1445–1461.
- Peterson, J.A., 1966. Glaciation of Frenchmans Cap-National Park, Papers and Proceedings of the Royal Society of Tasmania, pp. 117–134.
- Ponader, K.C., Potapova, M.G., 2007. Diatoms from the genus *Achnanthidium* in flowing waters of the Appalachian Mountains (North America): ecology, distribution and taxonomic notes. *Limnologica - Ecol. Manag. Inland Waters* 37, 227–241.
- R Development Core Team, 2014. In: *R: A Language and Environment for Statistical Computing*, 3.1.1. R Foundation for Statistical Computing, Vienna, Austria.
- Rees, A.B.H., Cwynar, L.C., Fletcher, M.S., 2015. Southern westerly winds submit to the ENSO regime: a multiproxy paleohydrology record from lake Dobson, Tasmania. *Quat. Sci. Rev.* 126, 254–263.
- Reid, M.A., Sayer, C.D., Kershaw, A.P., Heijnis, H., 2007. Palaeolimnological evidence for submerged plant loss in a floodplain lake associated with accelerated catchment soil erosion (Murray River, Australia). *J. Paleolimnol.* 38, 191–208.
- Renberg, I., Korsman, T., Anderson, N.J., 1993a. A temporal perspective of lake acidification in Sweden. *Ambio* 22, 264–271.
- Renberg, I., Korsman, T., Birks, H.J.B., 1993b. Prehistoric increases in the pH of acid-sensitive Swedish lakes caused by land-use changes. *Nature* 362, 824–827.
- Robinson, C.T., Rushforth, S.R., 1987. Effects of physical disturbance and canopy cover on attached diatom community structure in an Idaho stream. *Hydrobiologia* 154, 49–59.
- Rørslett, B., Brettm, P., 1989. The genus *Isoëtes* in Scandinavia: an ecological review and perspectives. *Aquat. Bot.* 35, 223–261.
- Sabbe, K., Vanhoutte, K., Lowe, R.L., Bergey, E.A., Biggs, B., Francoeur, S., Hodgson, D., Vyverman, W., 2001. Six new *Actinella* (Bacillariophyta) species from Papua New Guinea, Australia and New Zealand: further evidence for widespread diatom endemism in the Australasian region. *Eur. J. Phycol.* 36, 321–340.
- Saros, J.E., Anderson, N.J., 2015. The ecology of the planktonic diatom *Cyclotella* and its implications for global environmental change studies. *Biol. Rev.* 90, 522–541.
- Saros, J.E., Northington, R.M., Anderson, D.S., Anderson, N.J., 2016. A whole-lake experiment confirms a small centric diatom species as an indicator of changing lake thermal structure. *Limnol. Oceanogr. Lett.* 1, 27–35.
- Saros, J.E., Stone, J.R., Pederson, G.T., Slemmons, K.E.H., Spanbauer, T., Schliep, A., Cahl, D., Williamson, C.E., Engstrom, D.R., 2012. Climate-induced changes in lake ecosystem structure inferred from coupled neo-and paleoecological approaches. *Ecology* 90, 2155–2164.
- Saros, J.E., Strock, K.E., McCue, J., Hogan, E., Anderson, J.N., 2014. Response of *Cyclotella* species to nutrients and incubation depth in Arctic lakes. *J. Plankton Res.* 36, 450–460.
- Saunders, K.M., Harrison, J.J., Hodgson, D.A., Jong, d.R., Mauchle, F., McMinn, A., 2013. Ecosystem impacts of feral rabbits on World Heritage sub-Antarctic Macquarie Island: a palaeoecological perspective. *Anthropocene* 3, 1–8.
- Saunders, K.M., Hodgson, D.A., McMinn, A., 2009. Quantitative relationships between benthic diatom assemblages and water chemistry in Macquarie Island lakes and their potential for reconstructing past environmental changes. *Antarct. Sci.* 21, 35–49.
- Saunders, K.M., Hodgson, D.A., McMurtie, S., Grosjean, M., 2015. A diatom–conductivity transfer function for reconstructing past changes in the Southern Hemisphere westerly winds over the Southern Ocean. *J. Quat. Sci.* 30, 464–477.
- Saunders, K.M., Roberts, S., Perren, B., Butz, C., Sime, L., Davies, S., Van Nieuwenhuyze, W., Grosjean, M., Hodgson, D., 2018. Holocene dynamics of the Southern Hemisphere westerly winds and possible links to CO₂ outgassing. *Nat. Geosci.* 11, 650–655.
- Sherman, B.S., Webster, I.T., Jones, G.J., Oliver, R.L., 1998. Transitions between *Aulacoseira* and *Anabaena* dominance in a turbid river weir pool. *Limnol. Oceanogr.* 43, 1902–1915.
- Simpson, G.L., 2018a. Modelling palaeoecological time series using generalized additive models. *Front. Ecol. Evolut. Paleoccol.* 6, 149.
- Simpson, G.L., 2018b. R Package: gratia. In: Simpson, G.L. (Ed.), *Ggplot-based Graphics and Other Useful Functions for GAMs Fitted Using mgcv*, 0.1–0 (Ggplot-based graphics and utility functions for working with GAMs fitted using the mgcv package).
- Simpson, G.L., Anderson, N.J., 2009. Deciphering the effect of climate change and separating the influence of confounding factors in sediment core records using additive models. *Limnol. Oceanogr.* 54, 2529–2541.
- Smith, H.G., Sheridan, G.J., Lane, P.N.J., Nyman, P., 2011. Wildfire effects on water quality in forest catchments: a review with implications for water supply. *J. Hydrol.* 396, 170–192.
- Smol, J.P., 2010. The power of the past: using sediments to track the effects of multiple stressors on lake ecosystems. *Freshw. Biol.* 55, 43–59.
- Spaulding, S., Esposito, R., Lubinski, D., Horn, S., Cox, M., McKnight, D., Alger, A., Hall, B., Mayernick, M., Whittaker, T., Yang, C., 2010. Antarctic Freshwater Diatoms. *McMurdo Dry Valleys LTER*, United States.
- Spaulding, S.A., Lubinski, D.J., Potapova, M., 2019. Diatoms of North America, United States.
- Stahle, L.N., Chin, H., Haberle, S., Whitlock, C., 2017. Late-glacial and Holocene records of fire and vegetation from cradle mountain National park, Tasmania, Australia. *Quat. Sci. Rev.* 177, 57–77.
- Steane, M.S., Tyler, P.A., 1982. Anomalous stratification behaviour of Lake Gorden, headwater reservoir of the lower Gorden river, Tasmania. *Mar. Freshw. Res.* 33, 739–760.
- Steinberg, C.E.W., 2003. Direct Effects on Organisms and Niche Differentiation, Ecology of Humic Substances in Freshwaters: Determinants from Geochemistry to Ecological Niches. Springer, Heidelberg, Germany.
- Tibby, J., Penny, D., Leahy, P., Kershaw, A.P., 2012. Vegetation and water quality responses to Holocene climate variability in Lake Purumbete, western Victoria. In: Haberle, S., David, B. (Eds.), *Peopled Landscapes: Archaeological and Biogeographic Approaches to Landscapes, Terra Australis*. ANU E Press, Canberra, pp. 359–374.
- Tyler, P.A., 1974. Limnological studies. In: Williams, W.D. (Ed.), *Biogeography and Ecology in Tasmania*. Dr. W. Junk b.v., Publishers, The Hague, Dordrecht, Netherlands, pp. 29–61.
- Vacht, P., Puusepp, L., Koff, T., Reitalu, T., 2014. Variability of riparian soil diatom communities and their potential as indicators of anthropogenic disturbances. *Est. J. Ecol.* 63, 168–184.
- van Dam, H., Suurmond, G., ter Braak, C.J., 1981. Impact of acidification on diatoms

- and chemistry of Dutch moorland pools. *Hydrobiologia* 83, 425–459.
- Vanhoutte, K., Verleyen, E., Vyverman, W., Chepurnov, V.A., Sabbe, K., 2004. The freshwater diatom genus *Kobayasiella* (Bacillariophyta) in Tasmania, Australia. *Aust. Syst. Bot.* 17, 483–496.
- Vyverman, W., Vyverman, R., Hodgson, D., Tyler, P., 1995. Diatoms from Tasmanian mountain lakes: a reference data-set for environmental reconstruction. In: The TASDIAT Diatom Training Set: a Systematic and Autoecological Study. Cramer, Berlin.
- Vyverman, W., Vyverman, R., Rajendran, V.S., Tyler, P., 1996. Distribution of benthic diatom assemblages in Tasmanian highland lakes and their possible use as indicators of environmental changes. *Can. J. Fish. Aquat. Sci.* 53, 493–508.
- Wetzel, R.G., 1992. Gradient-dominated ecosystems: sources and regulatory functions of dissolved organic matter in freshwater ecosystems. *Hydrobiologia* 229, 181–198.
- White, I., Wade, A., Worthy, M., Mueller, N., Daniell, T., Wasson, R., 2006. The vulnerability of water supply catchments to bushfires: impacts of the January 2003 wildfire on the Australian Capital Territory. *Aust. J. Water Resour.* 10, 179–194.
- Whitlock, C., Larsen, C., 2001. Charcoal as a fire proxy. In: Smol, J.P., Birks, H.J.B., Last, W.M. (Eds.), *Tracking Environmental Change Using Lake Sediments. Volume 3: Terrestrial, Algal, and Siliceous Indicators*. Kluwer Academic Publishers, Dordrecht, The Netherlands, pp. 75–97.
- Wood, S., 2016. Package: Mgcv, Mixed GAM Computation Vehicle with GCV/AIC/REML Smoothness Estimation, vol. 1, pp. 8–15.
- Wood, S.N., 2011. Fast stable restricted maximum likelihood and marginal likelihood estimation of semiparametric generalized linear models. *J. R. Stat. Soc.: Stat. Methodol. Ser. B* 73, 3–36.
- Wood, S.W., Bowman, D.M.J.S., 2012. Alternative stable states and the role of fire–vegetation–soil feedbacks in the temperate wilderness of southwest Tasmania. *Landsc. Ecol.* 27, 13–28.
- Yee, T.W., Mitchell, N.D., 1991. Generalized additive models in plant ecology. *J. Veg. Sci.* 2, 587–602.